

2
100

NAVAL POSTGRADUATE SCHOOL Monterey, California

AD-A268 938



DTIC
ELECTE
SEP 08 1993
S B D

THESIS

CLOSE-COUPLED OSCILLATING
CANARD EFFECTS ON POST-STALL
LIFT ENHANCEMENT

by

Douglas G. Mc Bane

June, 1993

Thesis Advisor:

Richard M. Howard

93-20718

Approved for public release; distribution is unlimited

93 3 00 041

REPORT DOCUMENTATION PAGE				
1a Report Security Classification: Unclassified		1b Restrictive Markings		
2a Security Classification Authority		3 Distribution/Availability of Report Approved for public release; distribution is unlimited		
2b Declassification/Downgrading Schedule				
4 Performing Organization Report Number(s)		5 Monitoring Organization Report Number(s)		
6a Name of Performing Organization Naval Postgraduate School		6b Office Symbol (if applicable) 31	7a Name of Monitoring Organization Naval Postgraduate School	
6c Address (city, state, and ZIP code) Monterey CA 93943-5000		7b Address (city, state, and ZIP code) Monterey CA 93943-5000		
8a Name of Funding/Sponsoring Organization		6b Office Symbol (if applicable)	9 Procurement Instrument Identification Number	
Address (city, state, and ZIP code)		10 Source of Funding Numbers		
		Program Element No	Project No	Task No
		Work Unit Accession No		
11 Title (include security classification) Close-Coupled Oscillating Canard Effects on Post-Stall Lift Enhancement				
12 Personal Author(s) Mc Bane, Douglas G.				
13a Type of Report Master's Thesis		13b Time Covered From To	14 Date of Report (year, month, day) June 1993	15 Page Count 97
16 Supplementary Notation The views expressed in this thesis are those of the author and do not reflect the official policy or position of the Department of Defense or the U.S. Government.				
17 Cosati Codes		18 Subject Terms (continue on reverse if necessary and identify by block number)		
Field	Group	Subgroup	Oscillating Canard, Close-Coupled Canard, Dynamic Stall	
19 Abstract (continue on reverse if necessary and identify by block number) The effects of an oscillating close-coupled canard on the canard/wing vortex interaction for increased lift enhancement were studied. Two test conditions were studied: the first with a model angle of attack of 22 deg. and the second of 34 deg. The canard was positioned at three mean deflection angles equal to 4, 7 and 10 deg. for the model angle of attack of 22 deg. and -4, -7 and -10 deg. for the model angle of attack of 34 deg. At each of the canard mean deflection angles, the canard was oscillated with amplitudes of ± 5 deg. and ± 10 deg. with reduced frequencies ranging from 0.046 to 0.232. Because of the small effects noted which were of the order of accuracy of the balance, only general trends are discussed. The trends indicate that for this particular model configuration and geometry, lift was decreased slightly with increasing canard frequency and amplitude. No lift-enhancement benefits were revealed during the study.				
20 Distribution/Availability of Abstract __ unclassified/unlimited <u>x</u> same as report __ DTIC users		21 Abstract Security Classification Unclassified		
22a Name of Responsible Individual Richard M. Howard		22b Telephone (include Area Code) 408 656 2870	22c Office Symbol AA/Ho	

Approved for public release; distribution is unlimited

CLOSE-COUPLED OSCILLATING
CANARD EFFECTS ON POST-STALL
LIFT ENHANCEMENT

by

Douglas G. Mc Bane
Lieutenant, United States Navy
B.S., Texas Tech University, 1984

Submitted in partial fulfillment
of the requirements for the degree of

MASTER OF SCIENCE IN AERONAUTICAL ENGINEERING

from the

NAVAL POSTGRADUATE SCHOOL

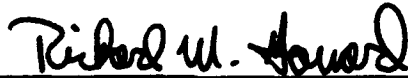
June, 1993

Author:

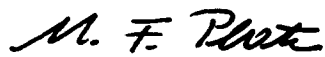


Douglas G. Mc Bane

Approved by:



Richard M. Howard, Thesis Advisor



Maximilian F. Platzer, Second Reader



Daniel J. Collins, Chairman
Department of Aeronautics and Astronautics

ABSTRACT

The effects of an oscillating close-coupled canard on the canard/wing vortex interaction for increased lift enhancement were studied. Two test conditions were studied: the first with a model angle of attack of 22° and the second of 34° . The canard was positioned at three mean deflection angles equal to 4° , 7° and 10° for the model angle of attack of 22° and -4° , -7° and -10° for the model angle of attack of 34° . At each of the canard mean deflection angles, the canard was oscillated with amplitudes of $\pm 5^\circ$ and $\pm 10^\circ$ with reduced frequencies ranging from 0.046 to 0.232. Because of the small effects noted which were of the order of accuracy of the balance, only general trends are discussed. The trends indicate that for this particular model configuration and geometry, lift was decreased slightly with increasing canard frequency and amplitude. No lift-enhancement benefits were revealed during the study.

DTIC QUALITY INSPECTED 1

Accession For	
NTIS GRA&I	<input checked="" type="checkbox"/>
DTIC TAB	<input type="checkbox"/>
Unannounced	<input type="checkbox"/>
Justification	
By _____	
Distribution/	
Availability Codes	
Dist	Avail and/or Special
A-1	

TABLE OF CONTENTS

I.	INTRODUCTION.....	1
	A. BACKGROUND.....	1
	B. DYNAMIC STALL.....	2
	C. CANARD CONFIGURED AIRCRAFT.....	3
	D. PREVIOUS STUDIES.....	4
	E. STATEMENT OF PURPOSE.....	7
II.	EXPERIMENT.....	9
	A. WIND TUNNEL.....	9
	B. STRAIN GAGE BALANCE AND TURNTABLE.....	12
	C. CANARD/WING MODEL.....	16
	D. DATA ACQUISITION HARDWARE AND SOFTWARE.....	17
	E. TEST CONDITIONS.....	19
III.	EXPERIMENTAL PROCEDURES.....	21
	A. PRE-RUN CALIBRATION.....	21
	B. DATA COLLECTION.....	24
IV.	DISCUSSION OF RESULTS.....	27
	A. MODEL AOA = 22° , AMPLITUDE = $\pm 5^\circ$	28
	B. MODEL AOA = 22° , AMPLITUDE = $\pm 10^\circ$	31
	C. MODEL AOA = 34° , AMPLITUDE = $\pm 5^\circ$	32
	D. MODEL AOA = 34° , AMPLITUDE = $\pm 10^\circ$	32
	E. SUMMARY OF RESULTS.....	33
V.	ERROR ANALYSIS.....	36
	A. UNCERTAINTY IN DYNAMIC PRESSURE (q).....	36

B. STATISTICAL SIGNIFICANCE OF DATA.....	38
C. DATA ACQUISITION UNCERTAINTY.....	39
VI. CONCLUSIONS AND RECOMMENDATIONS.....	42
REFERENCES.....	44
APPENDIX A: MODEL DESIGN.....	46
APPENDIX B: BALANCE CALIBRATION.....	53
APPENDIX C: DATA ACQUISITION PROGRAM.....	69
APPENDIX D: EXPERIMENTAL DATA.....	77
INITIAL DISTRIBUTION LIST.....	90

ACKNOWLEDGEMENTS

The completion of this work was done swiftly and without serious problems because of the efforts of many people, some of whom I have had direct contact with and some whom I have not. I would like to send a special thank you to the people that directed and supported me directly.

- Mr. Don Meeks whose tireless effort resulted in a canard oscillation-mechanism that worked perfectly, enabling me to gather my data without problems.

-Mr. Ron Ramaker whose swift completion of the main-wing for the model enabled me to piece together my experimental setup early enough to correct any potential problems.

- LT Dean C. Schmidt who had every conceivable problem when he tried to complete this experiment and worked out solutions to most of them so that I could perform the experiment without problems.

- Professor Richard M. Howard whose discerning eye, infinite patience and guidance helped me make sense out of the results I obtained.

- To my Father, who always wanted me to go to graduate school, but did not live to see me graduate.

And finally, I would like to thank my wife Patti and daughter Shannon for their patience and support.

Thank You All!!

I. INTRODUCTION

A. BACKGROUND

With the continued technological advances and human physiological limitations becoming the edge of the operating envelope in air combat, innovative technologies must be developed in order to maintain a decided advantage over potential adversaries. This advantage includes the ability to engage an adversary and bring the nose to bear upon the adversary as quickly as possible. According to Dornheim [Ref. 1], [the development of] "All aspect weaponry meant that tail chase tactics no longer had to dominate short range combat. Instead just pointing at the adversary is sufficient". As McAtee [Ref. 2] states, "the decision to engage is based on time to kill which has dropped considerably since World War II". This type of maneuvering facilitates the use of all-aspect weapons where the bottom line is being the first one to maneuver the aircraft into the weapons envelope. Current technologies being investigated to achieve these goals are thrust vectoring and post-stall lift enhancement utilizing a close-coupled canard. Thrust vectoring is being studied on the X-31 fighter aircraft, and the SAAB Viggen is generally credited as the first operational aircraft to successfully incorporate a close-coupled canard with a delta wing. According to Herbst [Ref. 3], "The combination of a delta wing

with a properly designed and integrated close-coupled canard furthermore improves maximum lift with less penalties of canard-wing interaction. At the same time, a canard can be used as a control device for optimum lift-to-drag throughout the flight envelope". Thus, the motivation for the study and development of post-stall lift enhancement and control is established.

Post-stall lift enhancement can be seen with many mechanisms including a close-coupled canard. However, "dynamic stall" as a post-stall lift enhancer, which is of interest for this research, has its roots in helicopter rotor dynamics.

B. DYNAMIC STALL

As Carr [Ref. 4] states, dynamic stall was first encountered "...when helicopter design engineers were unable to predict the performance of high speed helicopters using conventional aerodynamics". This phenomenon was also found in the flow over insect wings, compressor blades and the like. When investigated it was discovered that the rapid pitching experienced by the retreating blade caused the shedding, from the leading edge (in accordance with the Biot-Savart law), of a strong dynamic-stall vortex which energized the boundary layer causing the flow to remain attached at angles of attack well beyond the static stall angle of attack for the airfoil. This phenomenon is transient in nature and the lift

enhancement generated by the dynamic-stall phenomenon discontinues as soon as the vortex passes downstream of the airfoil. Carr [Ref. 4] studied dynamic stall of two-dimensional airfoils in detail and stated that "the need for basic research in three-dimensional dynamic stall effects, compressibility effects on dynamic stall and positive control of unsteady separated flow as well as other fundamental areas of unsteady aerodynamics" needs to be conducted. Carr [Ref. 4] also reviewed previous research on dynamic stall and found that free-stream Mach number as well as mean angle of attack, pitch-axis location, amplitude and frequency of oscillation affect dynamic stall.

C. CANARD CONFIGURED AIRCRAFT

Lacey [Ref. 5] performed extensive studies on close-coupled-canard location, sweep angle and size with respect to the main wing to maximize constructive interference and to ultimately increase lift. Results presented in Reference 5 indicate that for favorable interference to occur, the 40% exposed root chord position of the canard must be placed within 1.5 wing chords of the wing quarter chord with the exposed trailing edge of the canard slightly forward of the exposed leading edge of the wing root. The canard must be placed above the wing with an optimum vertical separation of 0.1 to 0.25 wing chords. Canard leading edge sweep should meet or exceed 60° . The area ratio (canard area/wing area =

(S_c/S_w) that provided the maximum lift coefficient, $S_c/S_w = 0.25$, was also the largest value tested, implying studies of larger area ratios may need to be conducted. Lift was decreased for small angles of attack in all cases, but lift was increased beyond the static stall angle of the wing alone at higher angles of attack.

Further research conducted by Er-El [Ref. 6] supported the conclusions of Lacey [Ref. 5] and added insight into the dynamics of the canard-wing interaction. Er-El [Ref. 6] stated, "The changes in the leading-edge-vortex trajectories due to the presence of the canard are evident in the pressure distributions. Comparison of the spanwise position of the suction peaks shows that in the wing/canard configuration these peaks are, in general, outboard to those in the wing alone configuration". Er-El [Ref. 6] also commented, "Evidently, the interaction between the wing and canard vortices in the aft section of the wing is stronger when the canard is highly swept due to its stronger vortices".

D. PREVIOUS STUDIES

Because dynamic stall is transitory in nature, creative engineering is necessary in order to exploit the benefits of dynamic stall on an as-needed and continuing basis. Because dynamic stall is created by the shedding of a strong leading-edge vortex following the rapid pitch of an airfoil, the airfoil must continually be pitched or oscillated to provide

the desired lift enhancement. Due to this pitch or oscillation requirement, the close-coupled-canard configuration is useful because the canard can be pitched in an oscillatory manner continuously to shed the leading-edge vortex necessary to possibly energize and reattach the flow over the main wing providing post-stall lift enhancement. Interest has been generated in determining whether a highly swept canard located optimally as determined by Lacey [Ref. 5] and oscillated continuously would help reattach the flow over the main wing, thus utilizing the dynamic stall phenomenon to enhance post-stall maneuverability.

Ashworth et al. [Ref. 7] obtained qualitative and quantitative data when the canard of an X-29-type half-body aircraft was sinusoidally oscillated. Smoke visualization showed the canard leading-edge vortex passing well above the main wing and the canard tip vortex being split by the main wing. Hot-wire measurements above and below the wing indicated that the flow velocity above the wing between 20% and 40% chord was slightly less than the free-stream velocity, indicating the existence of a separation bubble. Below the wing the velocity was essentially the free-stream value. No lift and drag measurements comparing the results of a non-oscillating canard and the results of an oscillating canard were taken.

Huyer et al. [Ref. 8] conducted similar studies where flow visualization and surface-mounted pressure transducers were used to characterize the flow fields over the trailing airfoil. This information was used to compute the pressure distributions as well as the normal and tangential force coefficients with the trailing airfoil at angles of attack of 10° and 20° . Huyer et al. [Ref. 8] analyzed the pressure distribution data and discussed the unsteady nature of the pressure distribution. Additionally, Huyer et al. [Ref. 8] discussed the canard dynamic-stall vortex effects on canard/wing interaction and stated "The production of the [dynamic stall] vortex did however, appear to energize the boundary layer and redirect the potential flow over the trailing airfoil. This phenomenon resulted in flow reattachment over the trailing airfoil surface at angles of attack far exceeding static stall angles." Huyer et al. [Ref. 8] however, does not compare the oscillating canard data to fixed canard data nor is there any lift or drag information presented.

Hebbar et al. [Ref. 9] utilized flow visualization to compare wing vortex burst location of an X-31-like fighter aircraft with a fixed and oscillating close-coupled canard. Reference 9 concludes that small amplitude and low frequency oscillations cause early vortex bursting whereas the small amplitude high frequency oscillations appear to delay vortex

bursting. It is worth noting that the reduced frequencies studied in Reference 9 ($k=1.7$ to $k=10.4$), are well above the reduced frequencies associated with dynamic stall ($k=0.1$ to $k=0.3$) studied in this research.

To this point previous research has focused on the qualitative aspects as well as the transitory effects of canard oscillation on canard/wing vortex interaction. Mabey et al. [Ref. 10] addresses an important point when he asks "can dynamic movement of the canard (about a constant mean setting) alter the mean flow on the canard and hence alter the mean flow on the wing?" This question is the focus of this research and quantitative measurements of lift and drag were taken.

E. STATEMENT OF PURPOSE

The purpose of this research was to build on previous research done by Kersh [Ref. 11] and Schmidt [Ref. 12] in considering the canard/wing interaction. Kersh [Ref. 11] studied the baseline lift and drag characteristics of a low-aspect-ratio wing/body model from low angles of attack to angles of attack beyond 36° . Additionally, Kersh [Ref. 11] studied the comparative lift enhancement using the same wing/body and a close-coupled canard for various wing/body angles of attack and various canard deflection angles.

The results of Kersh's [Ref. 11] studies were used to determine the test conditions studied by Schmidt [Ref. 12]

based on the maximum lift enhancement obtained with the close-coupled canard configuration. Schmidt [Ref. 12] obtained lift and drag measurements comparing the difference between tests in which a fixed canard and an oscillating canard were used to determine whether significant increases in lift could be obtained due to the dynamic-stall vortex effects on the canard/wing vortex interaction. Schmidt [Ref. 12] had significant difficulties with his experimental setup and the canard-oscillating mechanism and was not able to examine the full range of test conditions desired. This research followed the recommendations of Schmidt [Ref. 12] for model improvement. Additionally, increased frequency and amplitude ranges were examined to complete the study of the effects of an oscillating close-coupled canard on post-stall lift enhancement.

II. EXPERIMENT

A. WIND TUNNEL

The Naval Postgraduate School (NPS) low-speed wind tunnel located in the basement of Halligan Hall, as shown in Figure 1, was utilized for this experiment. As discussed in the NPS Laboratory Manual for Low Speed Wind Tunnel Testing [Ref. 13], the wind tunnel is 64 feet in length and varies in width between 21.5 and 25.5 feet. It is powered by a 100-horsepower electric motor connected to a four-speed International truck transmission. The transmission connects to a three-blade variable-pitch fan capable of providing test section velocities approaching 200 miles per hour. Directly downstream of the fan are eight flow straighteners to reduce turbulence and swirl. The flow passes through turning vanes at each of the four 90° turns that complete the wind tunnel circuit. In the settling chamber, two fine-wire turbulence screens six inches apart are installed to help provide smooth test section flows. The test section has a cross sectional area of approximately 10 square feet (45 inches wide and 32 inches high) and is approximately four feet long. The contraction ratio between the settling chamber and the test-section is 10:1. Test-section lighting and a reflection plane located in the test section reduce the usable cross-sectional

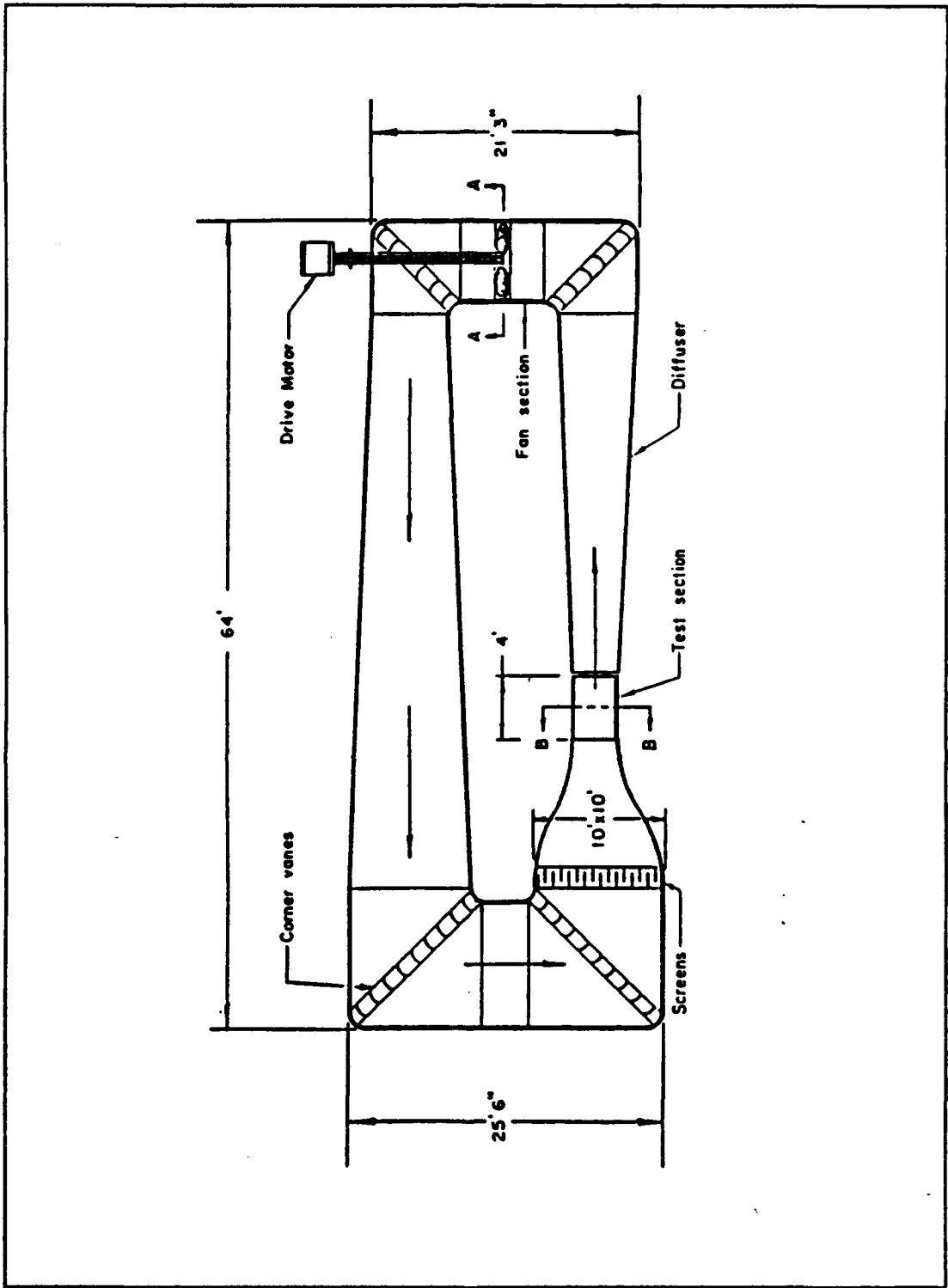


Figure 1: NPS Low Speed Wind Tunnel

area to approximately 9.88 square feet. The turbulence intensity in the test section is about 0.2% and a 1/500 tunnel diameter breather slot is installed just downstream of the test section for pressure recovery due to tunnel leakage. Temperature is measured using a dial thermometer with the probe located in the settling chamber. Test section dynamic pressure (q) is determined using a water-filled micromanometer whose readout is in centimeters of water. The settling chamber and the test-section each have a set of four wall-mounted static pressure taps with each set of four connected to individual common manifolds and then to the micromanometer. The resolution of the micromanometer was approximately equal to ± 0.1 cm. H_2O and the micromanometer could be zeroed to compensate for evaporation. Additionally, a digital pressure transducer was used for backup. The ΔP reading was converted to dynamic pressure using a calibration equation from Kersh [Ref. 11] as shown in Equation (1). Test section velocity was calculated using Bernoulli's equation and the definition of dynamic pressure, Equation (2).

$$q = 2.047 * (-0.026749 + 1.1149 \Delta P) \quad (1)$$

$$V = \sqrt{\frac{q}{1/2 * \rho}} \quad (2)$$

With the variables defined as follows:

ρ = Density (slugs/ft³)

ΔP = Micromanometer reading (cm. H₂O)

q = Dynamic pressure ($q = 27.33 \text{ lbf/ft}^2$)

V = Velocity (ft/s)

1.1149 = Tunnel calibration factor

2.047 = Conversion factor for cm. H₂O to lbf/ft²

-0.02675 = Tunnel calibration intercept

The wind tunnel calibration factor and tunnel calibration intercept correct micromanometer readings of ΔP in the range tested (3 - 12 cm. H₂O) to the actual test-section dynamic pressure. During calibration the actual test-section dynamic pressure was measured by a pitot-static probe placed in the test-section. The results were plotted against the micromanometer readings, and with the assumption of a linear relationship between the pitot-static probe and micromanometer readings, a slope (tunnel calibration factor) and a Y-intercept (tunnel calibration intercept) were calculated using a linear regression analysis as discussed in Yuan [Ref. 14] and Kersh [Ref. 11].

B. STRAIN GAGE BALANCE AND TURNTABLE

As discussed in Schmidt [Ref. 12], the external strain-gage balance was originally built by NPS personnel in 1974. It was designed to measure normal and axial forces as well as normal and axial moments. The balance was capable of

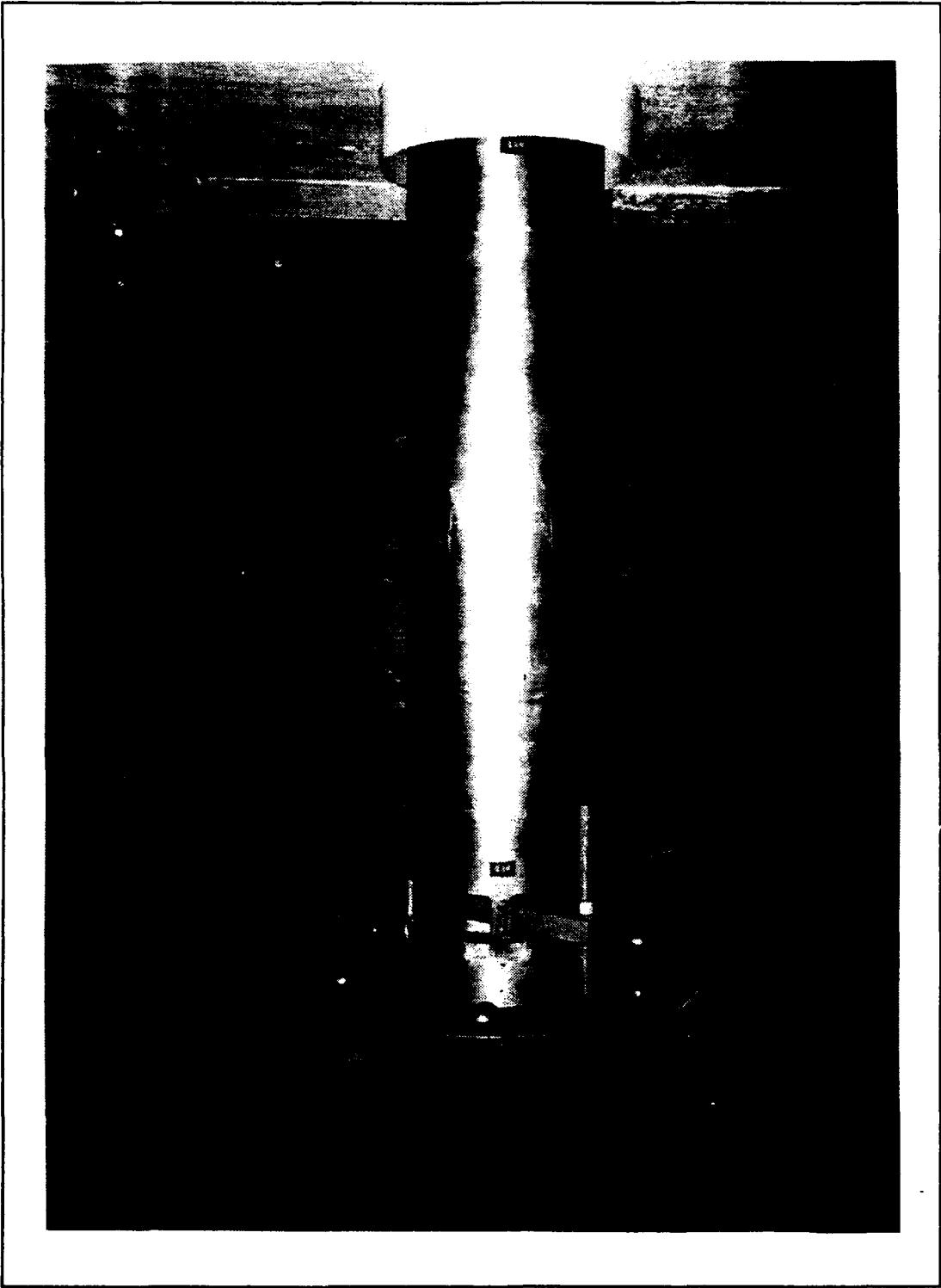


Figure 2: Strain Gage Balance

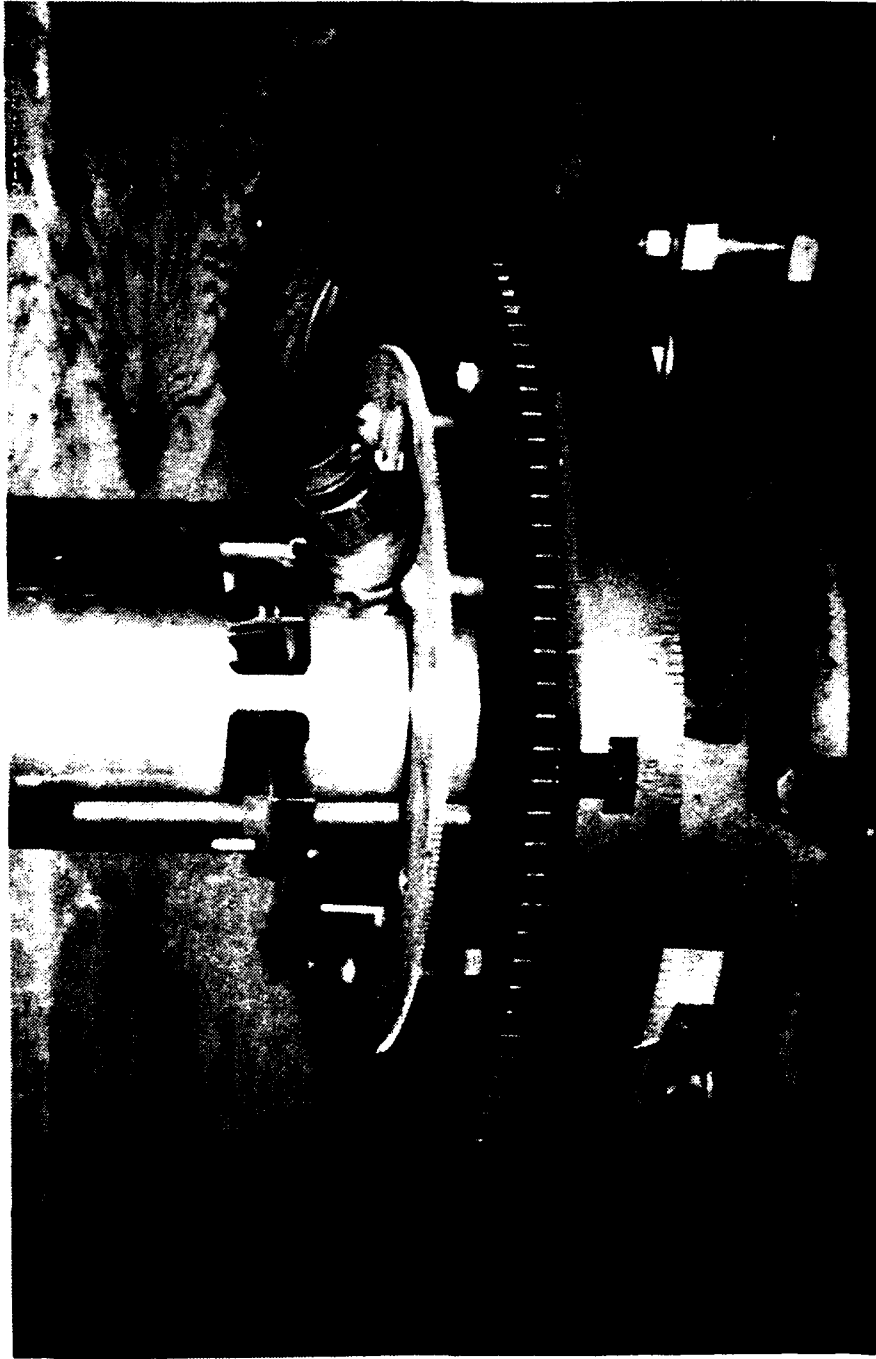


Figure 3: Balance Base and Markings

measuring forces up to 150 lbf and each of the four strain-gage bridge-circuits had four active legs with automatic temperature compensation. The forces and moments were measured by a pair of orthogonally-mounted strain-gages cemented on the flexure links of the balance column and were separated by a vertical distance of 26.5 inches (see Figure 2). The balance and turntable was capable of rotation from -18° to $+200^{\circ}$ relative to the tunnel centerline and rotation was controlled remotely by an electric motor (see Figure 3). The base of the balance was marked in degrees so that the operator could determine the angle of attack of the balance in relation to the tunnel centerline (see Figure 3). When the tunnel was in operation the forces and moments generated by the model translated into voltage readings on each of the four strain-gage bridge-circuits. These voltages were sent to the data acquisition system (discussed in section D. of this chapter) and the normal and axial forces were resolved into lift and drag and stored on floppy disc. The model (discussed in Appendix A.) was mounted to the reflection plane with 1/8-inch spacers to prevent the model from rubbing on the reflection plane when the angle of attack was changed (see Figure 4). The turntable had a 1/8-inch gap between itself and the reflection plane to allow the balance to deflect under loading (see Figure 4). The balance was calibrated before use to ensure accurate measurements as well as to verify that the

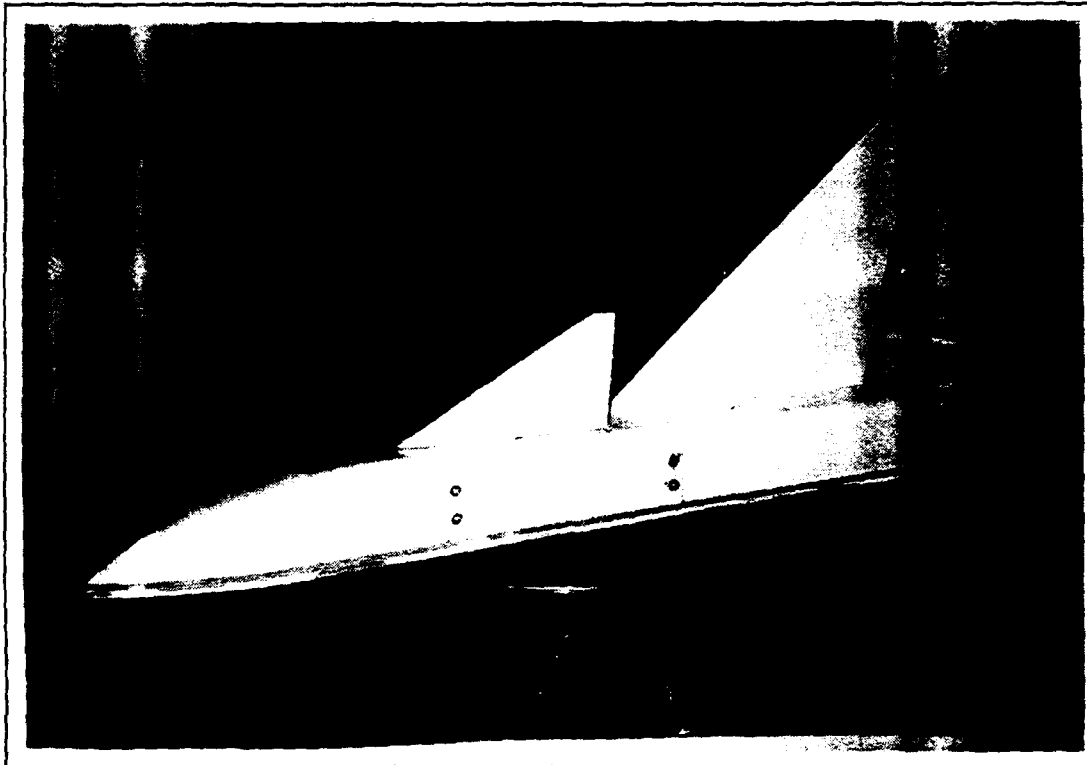


Figure 4: Turntable and Model

strain-gage bridge-circuits responded linearly to loading. The calibration process is discussed in detail in Appendix B.

C. CANARD/WING MODEL

The canard/wing model (see Figure 5) was a half-body made from mahogany and aluminum and mounted to an aluminum plate which mounted directly to the balance turntable (see Figure 4). The model was a generic fighter-type aircraft with a close-coupled canard and low-aspect-ratio wing (see Figure 5). The model consisted of three parts including the ogive nose, which was permanently mounted to the aluminum base. The second section was the canard-body section which housed the

canard oscillation mechanism and motor. On the top of the second section where the canard was mounted was a scale so that the canard mean deflection angle with respect to the fuselage centerline as well as the canard amplitude could be determined. The third section or aft-section contained the wing which was bolted to the aft body from the inside and enclosed the pick-up for the frequency counter used to determine the canard-oscillation frequency. The model design is described in detail in Appendix A.

D. DATA ACQUISITION HARDWARE AND SOFTWARE

Each strain-gage bridge had an individual signal-conditioner that provided the bridge excitation voltage (+10.0 volts) and a span zero (0.0 volts) so that the bridge could be balanced before use. The output from each bridge circuit was sent to a Pacific^o 8256 low-noise amplifier with the gain set at 1000. The outputs from the amplifiers were sent to and processed by a National Instruments^o MC-MIO-16L-9 12-bit multi-function board. The MC-MIO-16L-9 has an analog-to-digital converter with a 9.0 μ sec. conversion time capable of 100 Kbytes/sec. The board had a digitation span of 4096 bits resulting in a 4.88-mvolt resolution as discussed in the MC-MIO-16L-9 user manual [Ref 15]. The outputs of the MC-MIO-16L-9 board were then sent to an IBM PS-2^o computer. A data-acquisition program written by Schmidt [Ref. 12] was modified and utilized for automatic data acquisition and reduction.

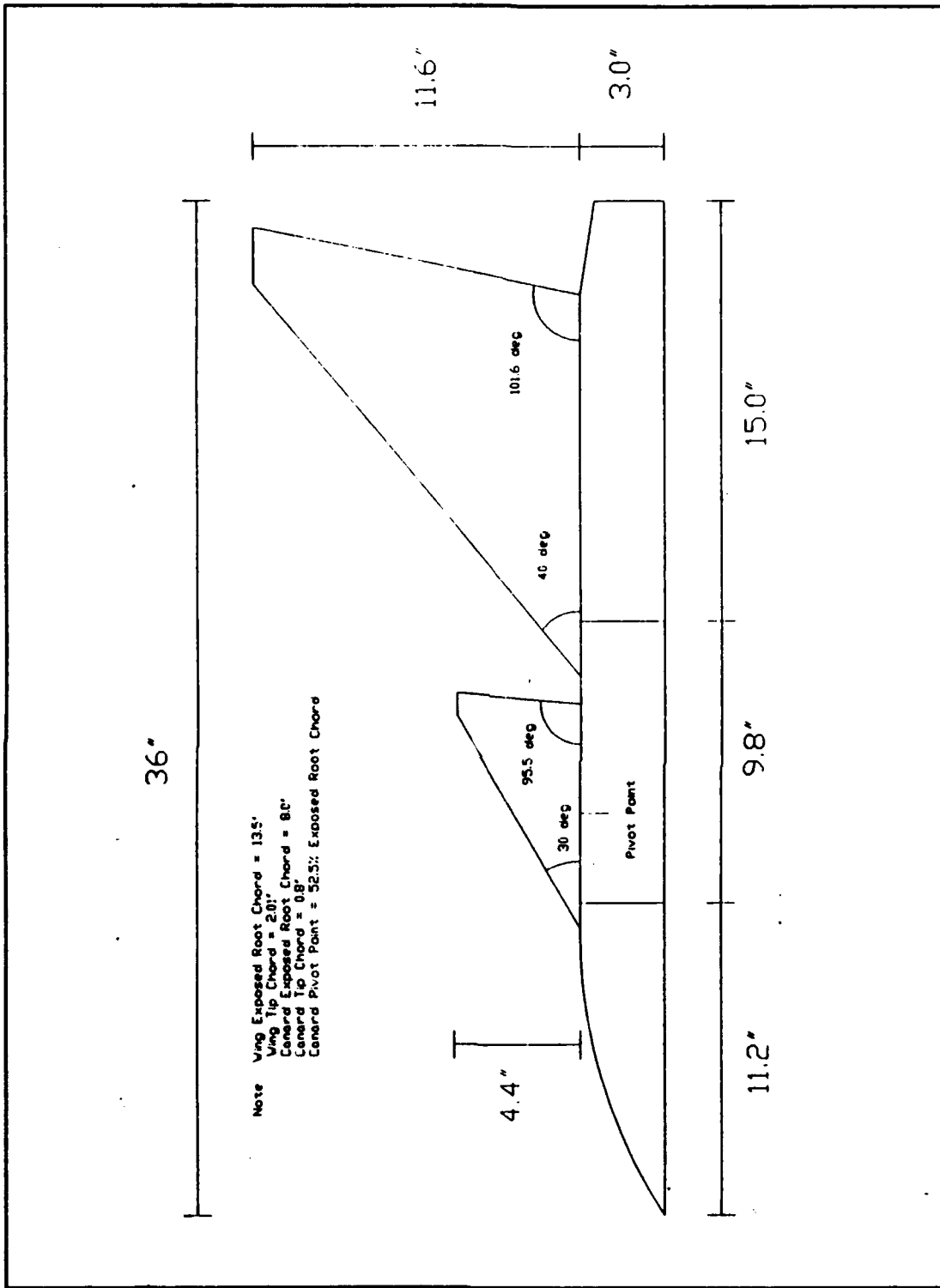


Figure 5: Model Configuration

The program was written using Microsoft QuickBasic 4.5⁰ implementing the MC-MIO-16L-9 board commands and compiled using National Instruments LabWindows⁰. The software was written so that each channel would be scanned 1000 times over a 2.25-second interval (444.44 Hz). The complete listing of the code and subroutines utilized can be found in Appendix C.

E. TEST CONDITIONS

The purpose of this experiment was to determine whether an oscillating close-coupled canard would provide significant increases in lift when compared to the results of a static close-coupled canard with the same configuration. The model configuration was based upon research done by Lacey [Ref. 5] in the early 1970's and the test conditions to be studied were based upon the results of Kersh [Ref. 11] and Schmidt [Ref. 12]. The results of Kersh [Ref. 11] indicate that for a model angle of attack of 22° , lift was maximized for a canard deflection angle of $+7^\circ$ and for a model angle of attack of 34° , lift was maximized for a canard deflection angle of -7° . These maximum values were bracketed for this experiment by adding or subtracting 3° to the canard deflection angle.

This research follows directly work done by Schmidt [Ref. 12] and incorporates model improvements discussed in Appendix A. The pivot-point for the canard was moved to 25% of the mean aerodynamic chord of the canard to reduce changes in pitching moment with canard deflection angle thus avoiding

problems encountered by Schmidt [Ref. 12]. For all the test conditions, a ΔP equal to 12 cm. H_2O was utilized which provided a dynamic pressure (q) of 27.33 lbf/ft².

The first model angle of attack (AOA) studied was +22°, with the canard at mean deflection angles equal to +4°, +7° and +10° with respect to the fuselage centerline. For each of these three test conditions, readings were taken with the canard fixed and with it oscillating at two amplitudes, ±5° and ±10°, at frequencies ranging from 5 hertz to 25 hertz in increments of 5 hertz. The results are presented in reduced frequencies and lift coefficients addressed in Chapter IV (Discussion of Results).

The second model AOA studied was +34°, with the canard at mean deflection angles equal to -4°, -7° and -10° with respect to the fuselage centerline. For each of these three test conditions, readings were taken with the canard fixed and with it oscillating at two amplitudes, ±5° and ±10°, with frequencies ranging from 5 hertz to 25 hertz in increments of 5 hertz. The results are presented in reduced frequencies and lift coefficients addressed in Chapter IV (Discussion of Results).

III. EXPERIMENTAL PROCEDURES

A. PRE-RUN CALIBRATION

Before any experiments were performed, the balance was calibrated and a calibration matrix was determined for use in the data acquisition program to resolve the strain-gage bridge outputs into lift and drag. The calibration procedure is discussed in detail in Appendix B and reviewed here briefly.



Figure 6: Cable and Pulley Setup

The turntable was aligned with the wind tunnel visually and the calibration rig was attached directly to the turntable. Two cable heights above the reflection plane of

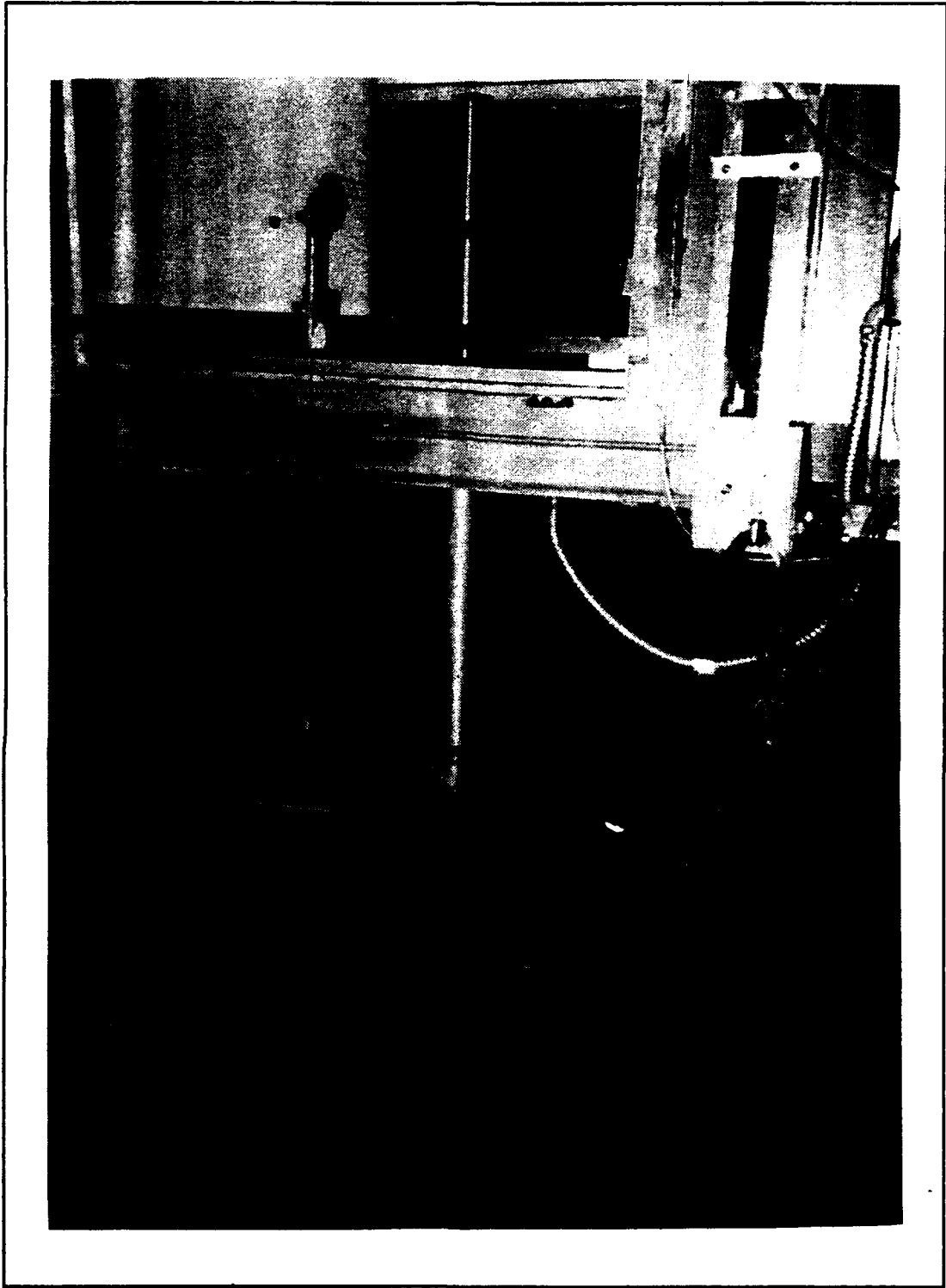


Figure 7: Calibration Rig

7.75 and 10.75 inches were utilized to resolve axial and normal moments. The cable was strung over a pulley and leveled with a sight-level and then attached to a weight-cage (see Figure 6 and Figure 7). Prior to beginning the calibration process the inputs to the Pacific[®] 8255 amplifiers were shorted. With the gain set to 1 the output screw was set to 0.0 ± 100.0 μ volts. The gain was then set to 1000 and the input screw was set to 0.0 ± 500.0 μ volts. The shorts were then removed and the bridge-circuit excitation voltage was set to 10.0 ± 0.05 volts and the span voltage set to 0.0 ± 0.05 volts at which point the calibration process was started. Weights were suspended in various increments up to 45 lbf from the cable to apply a known load to the balance and turntable. This was repeated for both cable heights; then the turntable was rotated 90° and the process repeated. The results were utilized to obtain the calibration matrix used during the test runs. The calibration matrix enabled the data acquisition program to resolve the strain-gage bridge-circuit outputs directly into lift and drag measurements. Because the span voltages were very difficult to zero and the amplifiers were prone to noise and drift at a gain of 1000 (see Error Analysis, Chapter V.), a tare reading was taken before each measurement and subtracted from the measurement. The software was written so that each channel would be scanned at 444.44 hertz for 2.25 seconds with the readings averaged, resulting

in a single value displayed and recorded to floppy disc. Each point was measured four times to ensure consistency and repeatability. The response from the strain-gage bridge-circuits proved to be linear as expected, and the calibration matrix obtained compares closely with that obtained by Schmidt [Ref. 12]. The calibration data can be found in Appendix B.

B. DATA COLLECTION

The test conditions as discussed in Chapter II, Section E, were utilized and are repeated for clarity:

1. Measured $\Delta P = 12$ cm. H_2O
2. Test section velocity = 150 ft/s (Approximately)
3. Model AOA = 22°
Canard Mean AOA = $+4^\circ, +7^\circ, +10^\circ$
Amplitude = $\pm 5^\circ, \pm 10^\circ$
Frequency = 0 - 25 hertz
4. Model AOA = 34°
Canard Mean AOA = $-4^\circ, -7^\circ, -10^\circ$
Amplitude = $\pm 5^\circ, \pm 10^\circ$
Frequency = 0 - 25 hertz

Since the canard/wing model had been significantly redesigned (see Appendix A.), no baseline validation of Schmidt's [Ref. 12] data was attempted.

A BK Precision[®] voltage supply with variable voltage and current settings was utilized to provide power to the canard-oscillation motor. Canard-oscillation frequency was measured

using a Monsanto^o Model 101A universal counter which counted the teeth of a gear mounted on the motor drive shaft. One revolution of the motor drive shaft was equal to one full-cycle of canard oscillation and by dividing the number displayed on the counter by the number of teeth on the sprocket, a frequency in hertz was obtained.

Because of difficulties encountered by Schmidt [Ref. 12], a set screw was installed in the model to maintain the mean deflection angle for the static test runs. After data were taken at the static test condition, the tunnel had to be shut down and the set screw removed before the canard was oscillated.

A pre-start checklist was utilized for each test condition and is as follows:

1. Operational amplifier input/output zeroed
 2. Excitation voltage set and span voltage zeroed
- Note: The first two procedures were completed only once before each block of tunnel runs (i.e. daily).
3. Tunnel temperature recorded.
 4. Atmospheric pressure recorded.
 5. Micromanometer zeroed.
 6. Model configuration set and checked (with set screw).
 7. Tare reading taken.
 8. Tunnel brought up to 12 cm. H₂O.
 9. Fixed-canard data point measured four times.

10. Tunnel shut down and set screw removed.
11. Tunnel brought up to 12 cm. H₂O.
12. Oscillating-canard data points measured four times each.
13. Zero reading taken after tunnel shut down.
14. Model reconfigured and steps 3 - 14 repeated.

The model and canard-oscillating mechanism performed extremely well (see Acknowledgments) and no difficulties were encountered in setting the test conditions desired or collecting data at the prescribed test conditions.

IV. DISCUSSION OF RESULTS

The following chapter covers all the test cases as discussed previously, and graphical results are presented in reduced frequencies which were calculated using Equation 1.

$$k = \frac{\omega * MAC_{canard}}{2 * V} \quad (1)$$

where:

ω = Canard oscillation frequency (radians/sec)

MAC_{canard} = 5.38 in. (0.4483 ft.)

V = Test section velocity (ft/s)

The lift and drag coefficient calculations were performed using Equations 2 and 3 below.

$$C_L = \frac{\text{lift}}{q * S} \quad (2)$$

$$C_D = \frac{\text{drag}}{q * S} \quad (3)$$

where:

lift = lift (lbf)

drag = drag (lbf)

S = Wing reference area to the fuselage centerline
(135.12 in² or 0.9383 ft²)

The reduced experimental data can be seen in Appendix D. The reduced data show the mean values at each test condition

as well as the standard deviation for each test condition. The mean values are the data used for the graphical presentations.

A. MODEL AOA = 22°, AMPLITUDE = ±5°

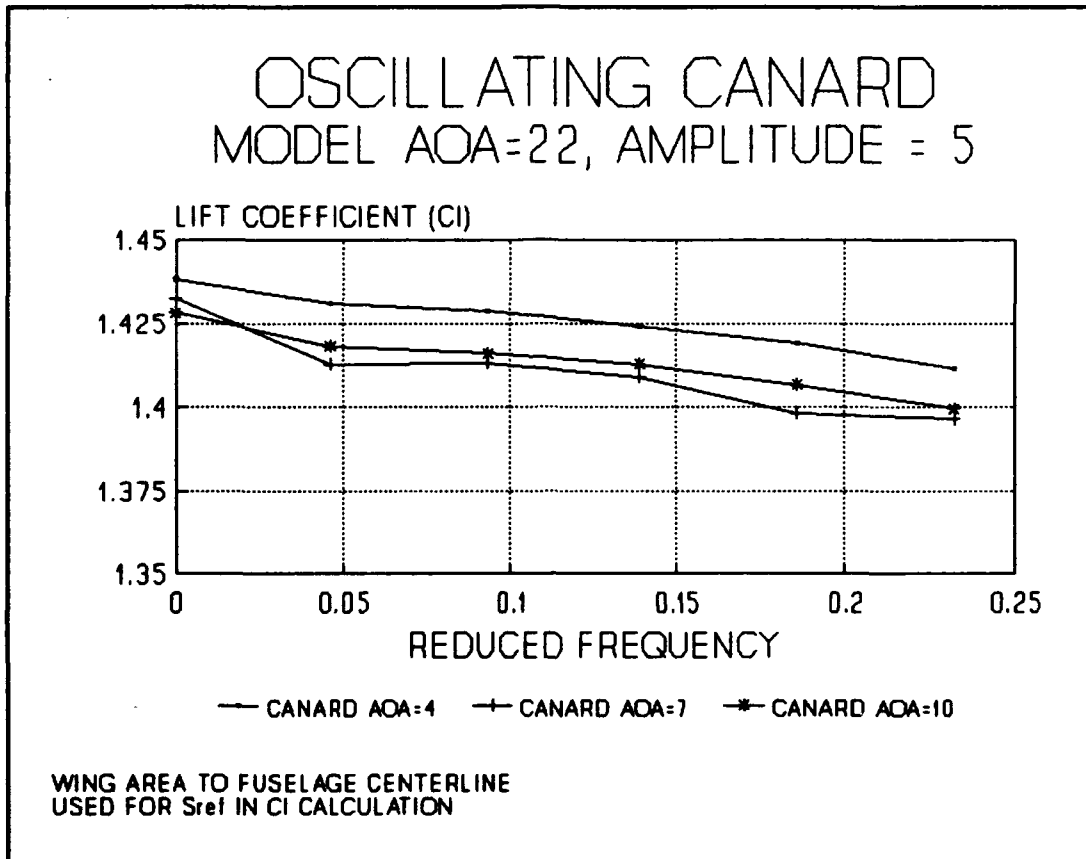
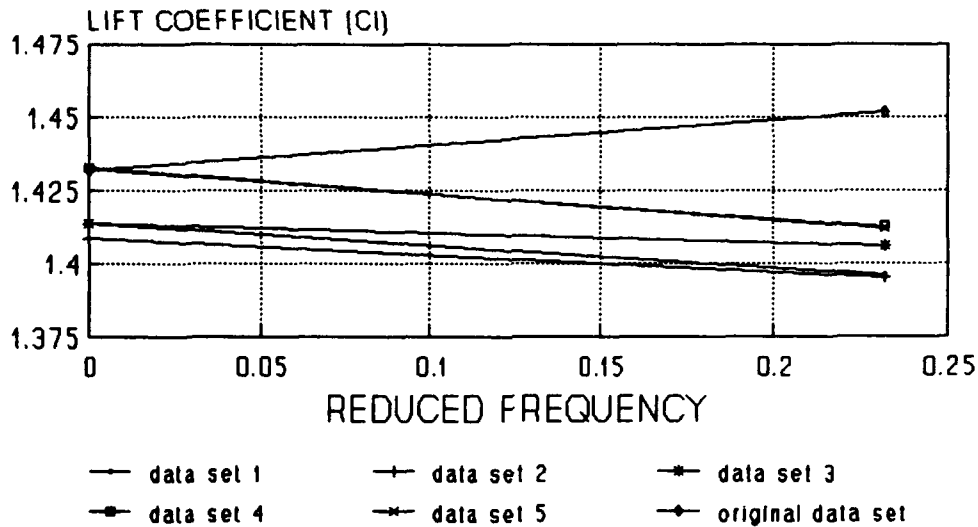


Figure 8: Model AOA = 22 deg.

Figure 8 shows the final results for the canard mean deflection angle equal to +4°, +7° and +10° with an amplitude of ± 5°. An initial examination of the reduced data showed the curve for a canard mean deflection angle of +7° indicating an increase in the lift coefficient at 5 hertz (k=0.046) when compared to the static case. Thereafter, as the canard

REPEATABILITY EXPERIMENT MODEL AOA = 22; CANARD AOA = 7



WING AREA TO FUSELAGE CENTERLINE
USED FOR S_{ref} IN C_l CALCULATION

Figure 9: Repeatability Experiment

oscillation frequency increased beyond 5 hertz ($k=0.046$) the lift coefficient decreased. Because of the uniqueness of this increase, the 5 hertz ($k=0.046$) data point was of interest; repeatability experiments were attempted without success. The repeatability experiment was conducted in the same manner as was the original experiment. For each test run the set screw was installed and data taken, then the tunnel was shut down and the set screw removed for the dynamic run. Figure 9 shows the results of the repeatability experiments where all but the original data reflect a decrease in the lift

coefficient at 5 hertz ($k=0.046$). The hypothesis for the discrepancy in results of the repeatability experiments lie in the nature of the experimental setup. As discussed previously, the static test had to be conducted with a set screw in the model to hold the canard mean deflection angle. After the static run the tunnel was shut down and the set screw removed. The tunnel was restarted and the dynamic readings were taken. Because the tunnel had to be shut down between the static and dynamic runs, there was an opportunity for a bias error to be introduced. The micromanometer utilized has a readability of approximately ± 0.1 cm. H₂O which equated to a ΔC_l equal to 0.01 (discussed in Error Analysis, Chapter V.). While ΔC_l equal to 0.01 is not a large change, it is on the same order of magnitude as the increase in the lift coefficient observed. Each data point had a statistical mean and standard deviation introducing other errors which are also discussed in detail in the Error Analysis chapter.

Because of the results obtained from the repeatability experiments, the decision was made to adjust the second data point at 5 hertz ($k=0.046$), as well as all subsequent data points from 10 to 25 hertz ($k=0.092 - 0.23$) downward by a ΔC_l equal to 0.039. The data in Appendix D reflect the original values obtained and not the corrected values; the values

displayed in Figure 8 were corrected for presentation and discussion purposes.

With the correction applied for the canard mean deflection angle equal to 7° , the test results indicate that the lift coefficient decreases steadily with an increase in canard frequency and the trend is consistent for all three test cases.

B. MODEL AOA = 22° , AMPLITUDE = $\pm 10^\circ$

Figure 10 shows the test results for canard mean

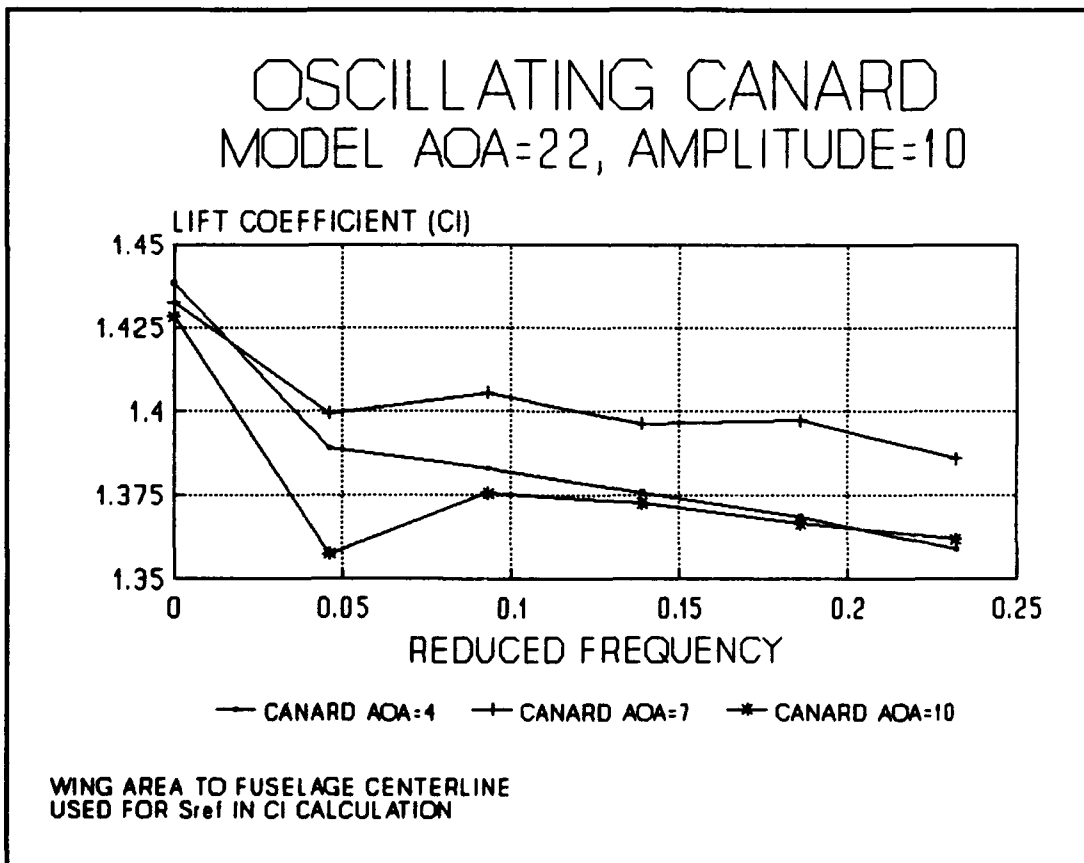


Figure 10: Model AOA = 22° deg.

deflection angles equal to $+4^\circ$, $+7^\circ$ and $+10^\circ$ with an amplitude of $\pm 10^\circ$. The same general trends as seen in Figure 8 are present in that the lift coefficient decreased with canard frequency regardless of canard mean deflection angle. It is interesting to note that the decrease in lift coefficient is more dramatic between the static and the first dynamic test condition, 5 hertz ($k=0.046$), when compared to the results of the $\pm 5^\circ$ amplitude case (Figure 8). The decrease in lift coefficient is consistent for all three test conditions.

C. MODEL AOA = 34° , AMPLITUDE = $\pm 5^\circ$

Figure 11 shows the test results for canard mean deflection angles equal to -4° , -7° and -10° with an amplitude of $\pm 5^\circ$. The lift coefficient decreased significantly between the static and first dynamic case, 5 hertz ($k=0.046$), with the canard mean deflection angle equal to -7° and -10° , then shows a relatively flat response to frequency for the remainder of the frequency range tested. For a canard mean deflection angle equal to -4° , Figure 11 shows an initial increase up to about 10 hertz ($k=0.092$) then a decrease with increased frequency for the remainder of the frequency tested.

D. MODEL AOA = 34° , AMPLITUDE = $\pm 10^\circ$

Figure 12 shows the test results for canard mean deflection angles equal to -4° , -7° and -10° with an amplitude of $\pm 10^\circ$. Similarly to the $\pm 5^\circ$ amplitude case, the canard mean deflection angles equal to -7° and -10° show a significant drop

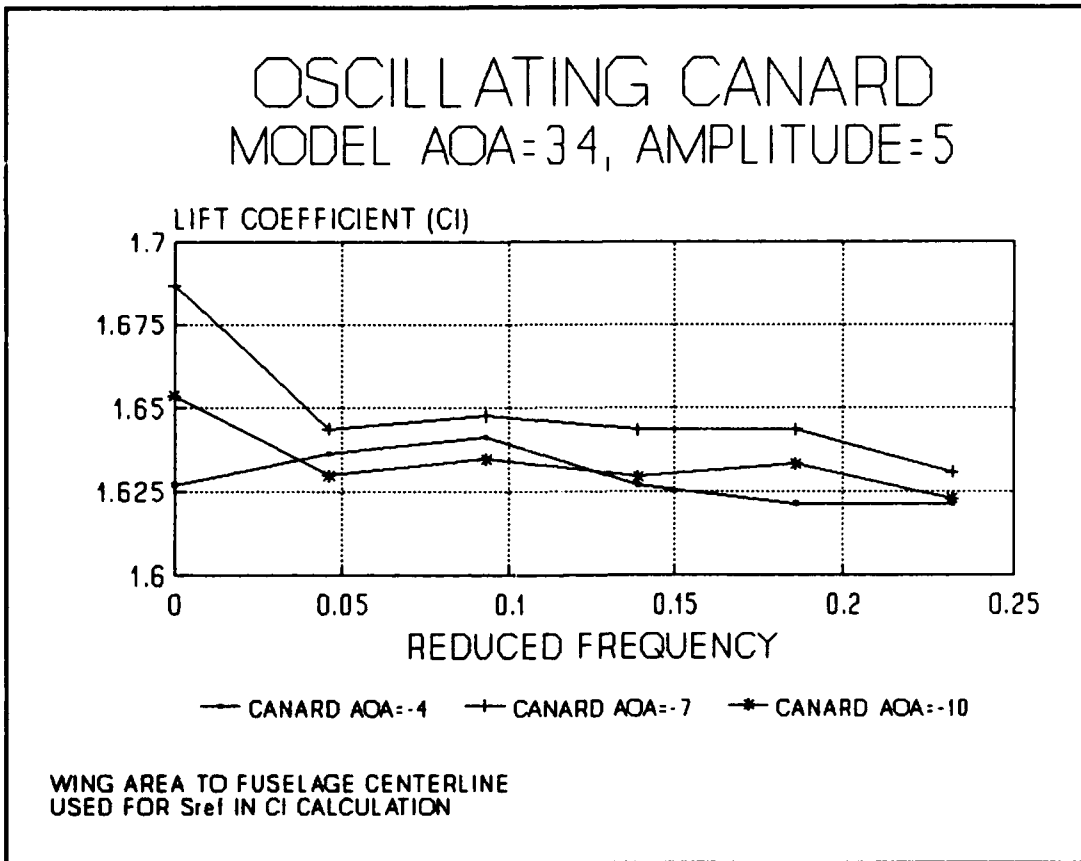


Figure 11: Model AOA = 34 deg.

between the static and first dynamic test case of 5 hertz ($k=0.046$). The results then show a relatively flat response throughout the remainder of the frequency range tested. For a mean canard deflection angle equal to -4° , the response is relatively flat throughout the frequency range tested.

E. SUMMARY OF RESULTS

For the model AOA equal to 22° , oscillating the canard seemed to have a negative effect on the lift coefficient. However, as is discussed in the Error Analysis chapter, the margin for error in the measurements is as large as the

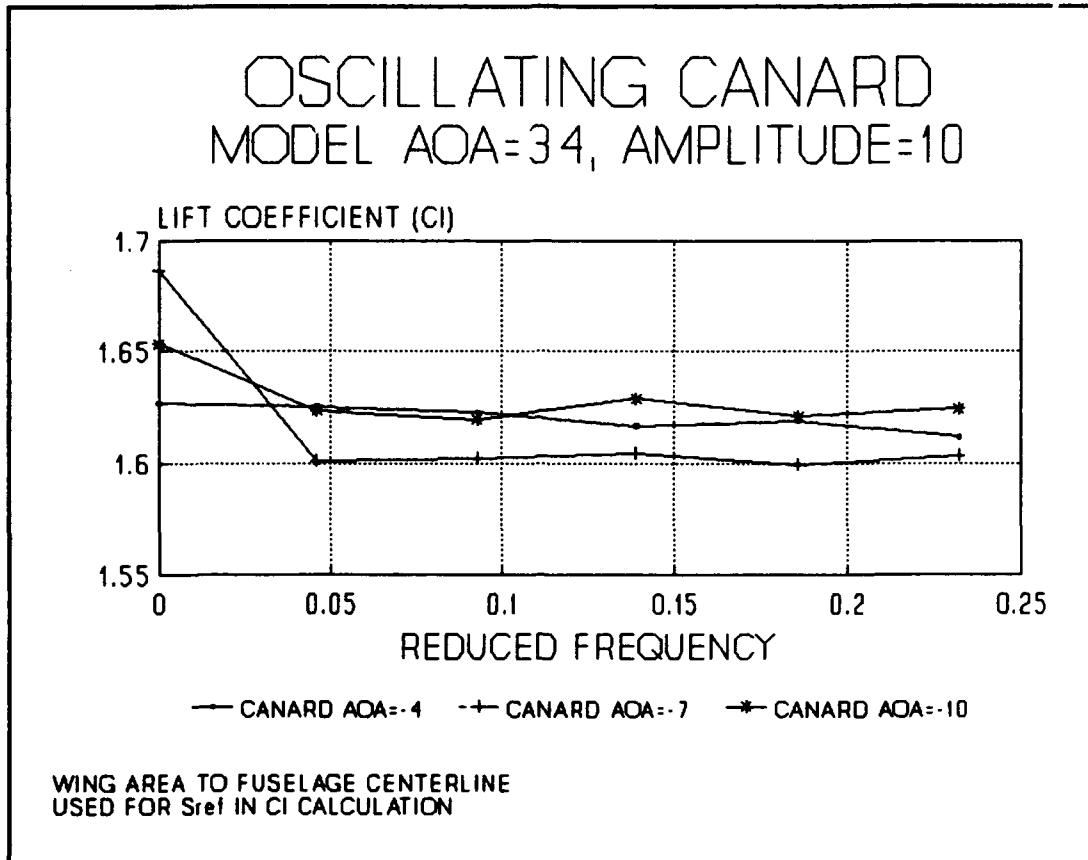


Figure 12: Model AOA = 34 deg.

relative difference in the measurements. This prohibits precise interpretation of the results, but the general trends seem to indicate that the lift coefficient is adversely affected when the canard is oscillated, and the canard dynamic stall vortex negatively affects the canard/wing vortex interaction and these negative effects are increased with increasing frequency. The increased canard amplitude of $\pm 10^\circ$ seemed to decrease the lift coefficient further because of the larger drop (between the static case and first dynamic case) than for the $\pm 5^\circ$ amplitude case. For the model AOA equal to

34°, the lift coefficient is adversely affected the most for canard mean deflection angles equal to -7° and -10°. The trend is relatively flat after the first dynamic case of 5 hertz ($k=0.046$), indicating relative frequency independence. For the canard mean deflection angle equal to -4°, a slight increase in lift coefficient for the amplitude equal to $\pm 5^\circ$ is seen up to 10 hertz ($k=0.092$), then a decrease for the remainder of the frequency range tested is noted. For the amplitude of $\pm 10^\circ$ there is a flat response for the entire frequency range tested. Care must be taken in interpreting the increase in lift coefficient for the canard mean deflection angle equal to -4° with the amplitude equal to $\pm 5^\circ$ because the increase is well within the statistical error limits as discussed in the Error Analysis chapter.

V. ERROR ANALYSIS

Because of the small magnitude of change between the measurements taken, particular attention had to be paid to error analysis. There appears to be three sources of error that will be discussed separately. The first source of error is the change in q (lbf/ft^2) due to the experimental setup requiring the tunnel be shut down between the static and dynamic test runs. The second source of error is in the data acquisition system and the third source is the statistical distribution of the data. Finally, no consideration of a fixed error or bias was considered because information on the relative differences between data points was sought, not absolute measurements.

A. UNCERTAINTY IN DYNAMIC PRESSURE (q)

A test was conducted to determine the tunnel sensitivity to lift coefficient variations with respect to changes in ΔP ($d\Delta C_l/d\Delta P$). Figure 13 shows a linear relationship between error in lift coefficient with respect to ΔP ($\text{cm. H}_2\text{O}$). There is a positive slope because the lift coefficient calculation is based on the assumption that ΔP , which equals $12 \text{ cm. H}_2\text{O}$, is constant which is consistent with the data reduction procedures. This linear relationship has a positive slope with a value of $d\Delta C_l/d\Delta P$ equal to 0.1185 . When the readability of the micromanometer is considered ($\Delta P = \pm 0.1 \text{ cm H}_2\text{O}$), it is evident that if for the static test case the

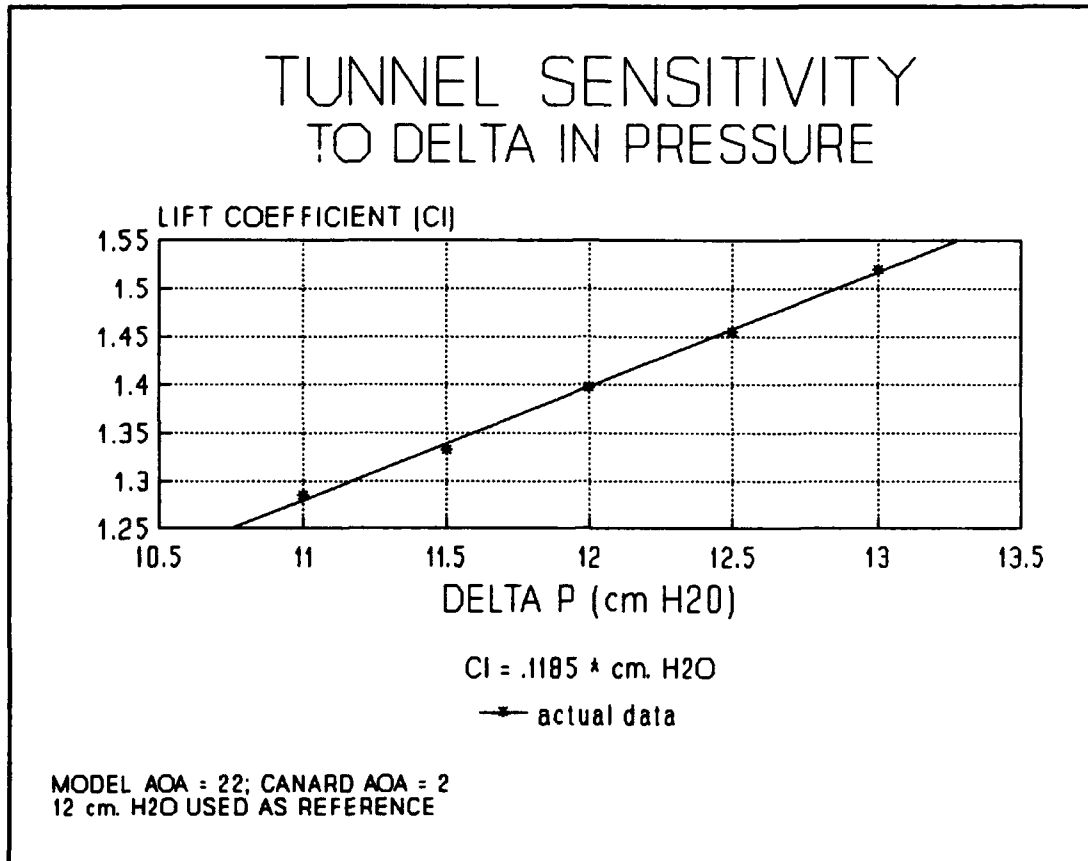


Figure 13:Tunnel Sensitivity

micromanometer were at the lower end of this interval and for the first dynamic case the micromanometer reading were at the high end of this interval an error in the lift coefficient (ΔC_l) as great as 0.02 is possible. This case is an extreme one and is unlikely but must be considered. Because the tunnel was not shut down between the dynamic runs (5 - 25 hertz, $k=0.046 - 0.23$) this error will not be present in the dynamic readings. Specifically, the relative difference between the dynamic readings would be accurate within the

statistical and data acquisition limitations and not subject to differences in q (lbf/ft²).

B. STATISTICAL SIGNIFICANCE OF DATA

Because of the small sample size of the data taken at each test condition, special statistical procedures were utilized to statistically legitimize the data. For a normal distribution with a large sample size the central limit theorem as discussed in McClave [Ref. 16] states, "If a random sample of "n" observations is selected from a population (any population), then, when "n" is sufficiently large, the sampling distribution of x_{bar} will be approximately a normal distribution. The larger the sample size, "n", the better will be the normal approximation to the sampling distribution of x_{bar} ." This theorem lays the foundation necessary for the calculation of the mean and standard deviation from which confidence intervals for the results can be established. But when presented with small sample sizes, work done by W.S. Gosset as discussed in McClave [Ref. 16], states that if a random sample is selected from a population with a normal distribution, the sampling distribution will be approximately normal. However, the variance of this small sample will have a greater uncertainty associated with it, so the t-statistic was developed. It accounts for larger uncertainty in both the mean and the variance due to the small sample size, so when developing confidence intervals they are much larger than for

the normal z-statistic as discussed in McClave [Ref. 16]. The t-statistic uses an "n-1" sample size and for a 95% confidence interval, the standard deviation is multiplied by 3.182 which compares to 1.96 for the z-statistic. The upper limit and the lower limit for the confidence interval as well as the variance can be found in the reduced experimental data in Appendix D. Confidence intervals as large as ± 0.03 can be found which are on the same order of magnitude as the changes in the lift coefficient observed.

C. DATA ACQUISITION UNCERTAINTY

Because of problems encountered by Kersh [Ref. 11] and Schmidt [Ref. 12], the data acquisition system was examined for its resolution capability. Additionally, it was known that the data acquisition outputs tended to drift cyclically with time. Figure 14 shows how the value of the lift coefficient drifted over a period of 1/2 hour. The tunnel was started and brought up to a ΔP equal to 12 cm. H_2O and data were taken every five minutes for 30 minutes. The ΔP data was plotted versus time and a linear regression was performed. The variance between the predicted value obtained from the regression equation and the actual value at a specific time were calculated to specify a confidence interval. The assumption that the drift in the system is linear for short periods of time can be seen to be reasonably accurate with a 90% confidence interval. The drift of the acquisition system

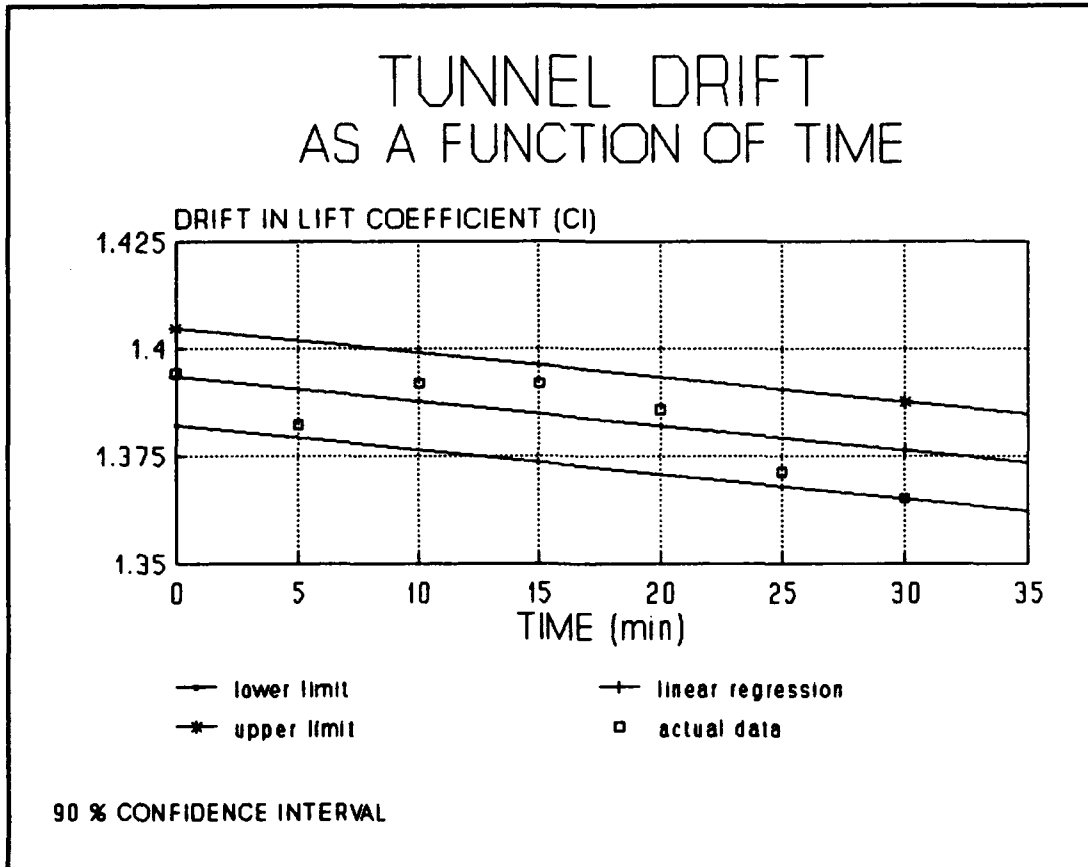


Figure 14: Tunnel Drift

was determined to be ΔC_l equal to -0.03 ± 0.01 per hour for this case. As a note, because the drift is oscillatory in nature, the drift-curve slope could just as easily have been positive and quite probably would have been if the drift were observed at some other time. The primary purpose of this discussion is to establish that the data acquisition system does in fact drift over the duration of a typical test run.

Because the drift is not linear and is more oscillatory over large periods of time, only a 30-minute period was examined because each test run performed between tare readings

took approximately 30 minutes. The source of drift was thought to be from amplifier output-voltage drift. This drift was not applied to any of the results discussed in Chapter IV.

Because of the unpredictable nature of the drift as well as the fact that the first type of error can be applied only between the first two data points, a standard uncertainty analysis as discussed in Holman and Gajda [Ref. 17] cannot be conducted. The importance of this discussion is evident when quantitative conclusions about the data are to be reached. Because the uncertainty is on the same small order of magnitude as the changes in lift coefficients, definite quantitative comparisons in the results cannot be made. However, general trends in the results can be noted to the effect that oscillating the canard provided no significant increase in lift as expected.

VI. CONCLUSIONS AND RECOMMENDATIONS

An oscillating close-coupled canard was studied to determine the effect on the canard/wing vortex interaction for increased lift enhancement. Two test conditions were studied: the first with a model angle of attack equal to 22° and the second equal to 34° . The canard was positioned at three mean deflection angles equal to 4° , 7° and 10° for the model angle of attack equal to 22° and -4° , -7° and -10° for the model angle of attack equal to 34° . At each of the canard mean deflection angles, the canard was oscillated with an amplitude equal to $\pm 5^\circ$ and $\pm 10^\circ$ with reduced frequencies, k , ranging from 0.046 to 0.232. The following conclusions were drawn from the test results.

- Because of the small effects noted which were of the order of accuracy of the balance, only general trends can be noted.

- The trends indicate that for this particular model configuration and geometry, lift was decreased slightly with increasing canard frequency and amplitude.

The following recommendations are made:

- Further studies of different model geometries with an oscillating canard need to be conducted. These studies should include varying the pivot-point of the canard, varying the dynamic pressure (q), and varying wing and canard geometries

as well as varying the frequency and amplitude of canard oscillation.

- The canard-oscillation mechanism needs to be modified so that the mean angle of attack can be maintained without a set screw. This will eliminate the necessity of shutting the tunnel down between the static and dynamic test runs, thus eliminating one source of error.

- The strain-gage balance and data acquisition system need to be replaced with a system capable of more accurate measurements. The balance itself is old and has been abused in the past, and the outputs of the bridge circuits will be in question as the balance is continually used.

- Flow visualization could be used to further understand the canard/wing vortex interaction.

REFERENCES

1. Dornheim, Michael A., *X-31 Flight Test to Explore Combat Agility to 70 Deg. AOA*, Aviation Week and Space Technology, pp. 38-41, March 1991.
2. McAtee, Thomas P., *Agility in Demand*, Aerospace America, Volume 26, Number 5, pp. 36-38, May 1988.
3. Herbst, W. B., *Future Fighter Technologies*, Journal of Aircraft, Volume 17, Number 8, pp.561-566, August 1980.
4. Carr, Lawrence W., *Progress in Analysis and Prediction of Dynamic Stall*, AIAA Journal, Volume 25, Number 1, pp.6-17, January 1988.
5. Lacey, David W., *Aerodynamic Characteristics of the Close-Coupled Canard as Applied to Low-to-Moderate Swept Wings*, Volume 1: General Trends, DTNSRDC-79/001, January 1979.
6. Er-El, J., *Effect of Wing/Canard Interference on the Loading of a Delta Wing*, Journal of Aircraft, Volume 25, Number 1, pp.18-24, January 1988.
7. Ashworth, J., Mouch, T., and Luttges, M., *Visualization and Anemometry Analyses of Forced Unsteady Flows about an X-29 Model*, AIAA Paper 88-2570, 1988.
8. Huyer, Stephen A., Luttges, Marvin W., *Unsteady Flow Interactions Between the Wake of an Oscillating Airfoil and a Stationary Trailing Airfoil*, AIAA Paper 88-2581, 1988.
9. Hebbar, Shesagiri K., Platzer Max F., Liu, Da-Ming, *Effect Of Canard Oscillations on the Vortical Flowfield of a X-31-Like Fighter Model in Dynamic Motion*, AIAA Paper 93-3427, 1993.
10. Mabey, D. G., Welsh, B. L., Pyne, C. R., *The Steady and Time-Dependent Aerodynamic Characteristics of a Combat Aircraft With a Delta or Swept Canard*, AGARD Conference Proceedings No. 465, October 1989.

11. Kersh, John M., Jr., *Lift Enhancement Using Close-Coupled Canard/Wing Vortex Interaction*, Master's Degree Thesis, Naval Postgraduate School, Monterey, CA, December 1990.
12. Schmidt, D. C., *Lift Enhancement Using a Close Coupled Oscillating Canard*, Master's Degree Thesis, Naval Postgraduate School, Monterey, CA, September 1992.
13. *Laboratory Manual for Low-Speed Wind Tunnel Testing*, Department of Aeronautics and Astronautics, Naval Postgraduate School, Monterey, CA, August 1989.
14. Yuan, Chi-Chung, *The Effects of Forebody Strakes on Asymmetric Vortices on a Vertically Launched Missile*, Master's Thesis, Naval Postgraduate School, Monterey, CA, September 1990.
15. *MC-MIO-16 User Manual*, National Instruments Corp., January 1989.
16. McClave, J.T., *Statistics for Business and Economics*, Dellen, 1988
17. Holman, J. P., and Gajda, W. J., Jr., *Experimental Methods for Engineers*, 5th Ed., McGraw-Hill Publishing Co., 1989.
18. Behrbohm, H., *Basic Low Speed Aerodynamics of Short Coupled Canard Configuration of Small Aspect Ratio*, SAAB Aircraft Co., Rept. SAAB TN-60, July 1965.

APPENDIX A: MODEL DESIGN

The model characteristics and design parameters were based on work previously done by Schmidt [Ref. 12], Kersh [Ref. 11] and Lacey [Ref. 5] and incorporated recommendations by Schmidt [Ref. 12] for the canard-oscillation mechanism.

A. GENERAL MODEL CONSIDERATIONS

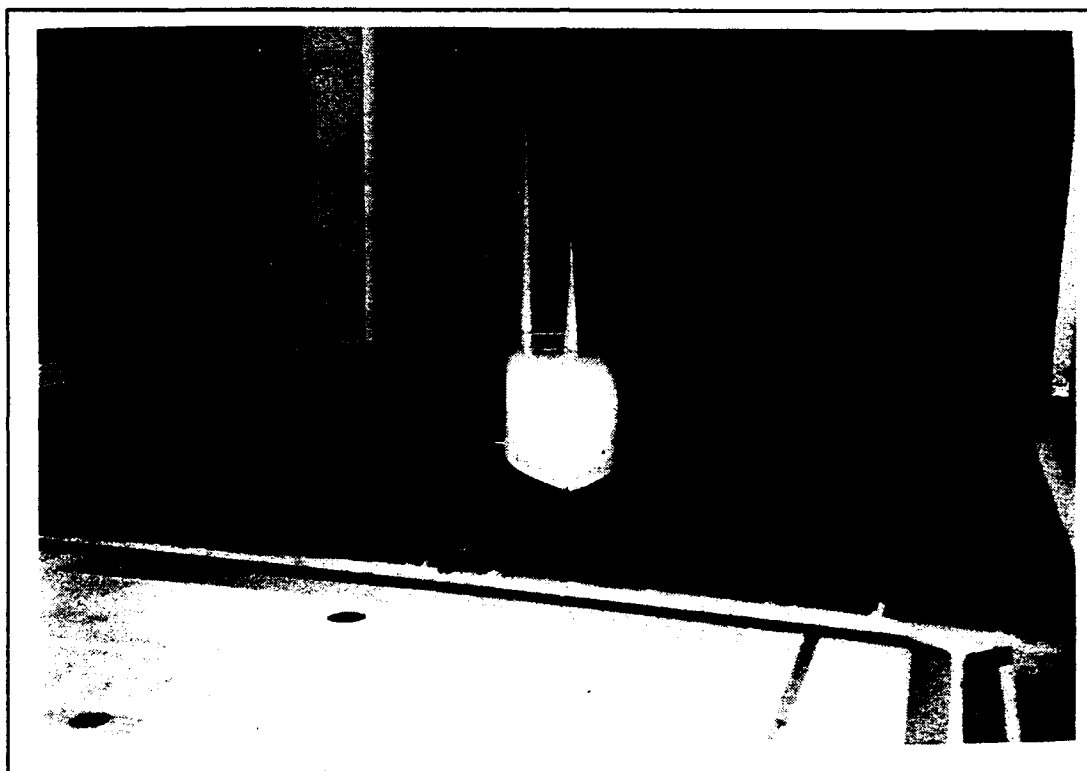


Figure A1: Model Configuration

The model can be seen in Figures A1 through A3 and utilizes the same fuselage as Kersh [Ref. 11] and Schmidt [Ref. 12]. An NACA 64A008 airfoil section was used for both the main wing and the canard. No attempt to trip the boundary

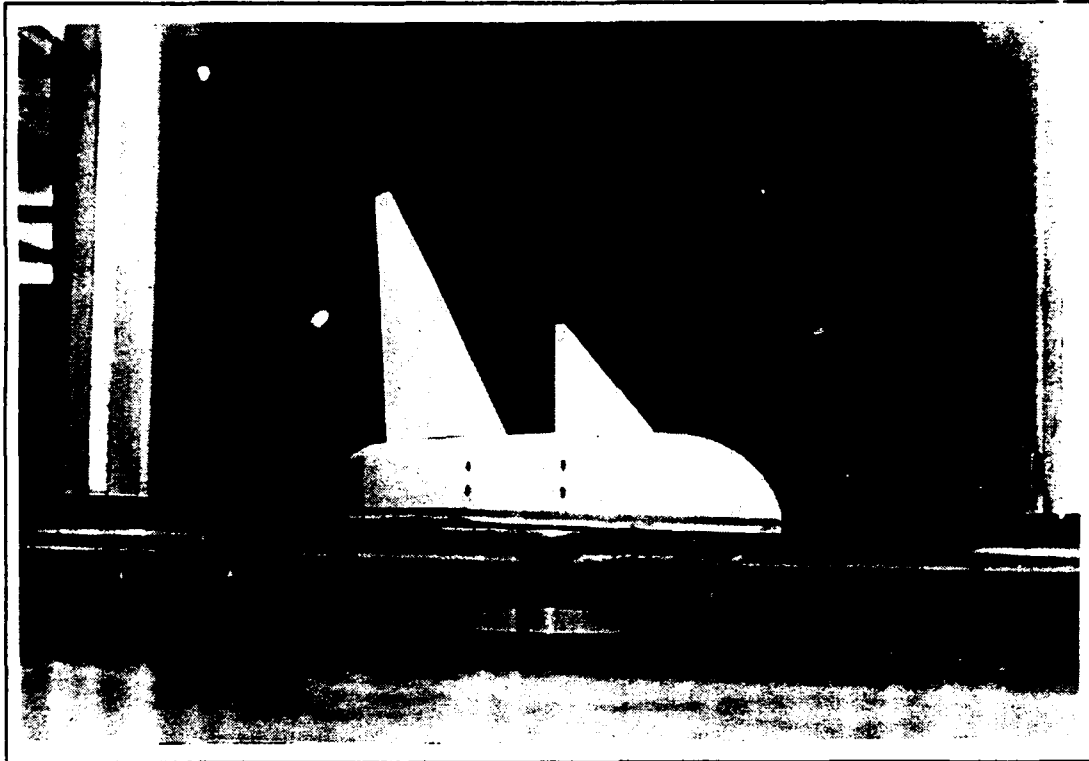


Figure A2: Model Configuration

existing aircraft airfoil shapes. The model was mounted to the balance turntable 17.18 inches back from the model tip of the ogive nose, and the model was 36 inches long. The fuselage was 4.5 inches wide and 3 inches high with a semi-span of 14.6 inches as measured from the reflection plane to the wing tip. The canard trailing edge did not overlap the wing as discussed in Lacey [Ref. 5] and the canard mean deflection angle was monitored by lines drawn on the model at the trailing edge of the canard in one-degree increments with the zero-degree deflection angle corresponding to the fuselage centerline.

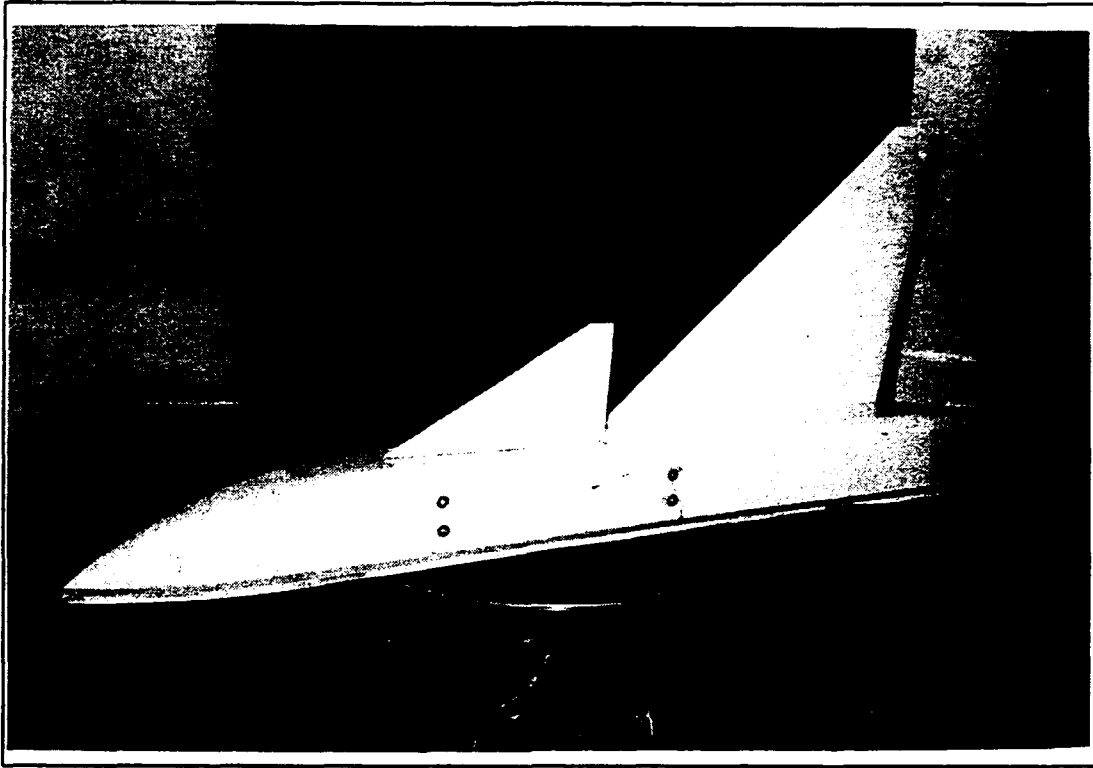


Figure A3: Model Configuration

the zero-degree deflection angle corresponding to the fuselage centerline.

B. CANARD MODIFICATIONS

The canard size and shape were determined by Kersh [Ref. 11] based upon work done by Lacey [Ref. 5] and Behrbohm [Ref. 18] and included a leading-edge sweep equal to 60° , taper ratio (λ) equal to 0.1 and an aspect ratio (AR) equal to 2 as calculated by Equations A1 and A2.

$$\lambda = \frac{C_t}{C_r} \quad (A1)$$

$$AR=2 \frac{b}{C_r(1+\lambda)}$$

(A2)

where:

b = Wingspan

C_r = Exposed root chord

C_t = Tip chord

The canard-oscillation mechanism was redesigned and reconfigured to handle the dynamic loadings created by canard oscillations as discussed by Schmidt [Ref. 12], and the

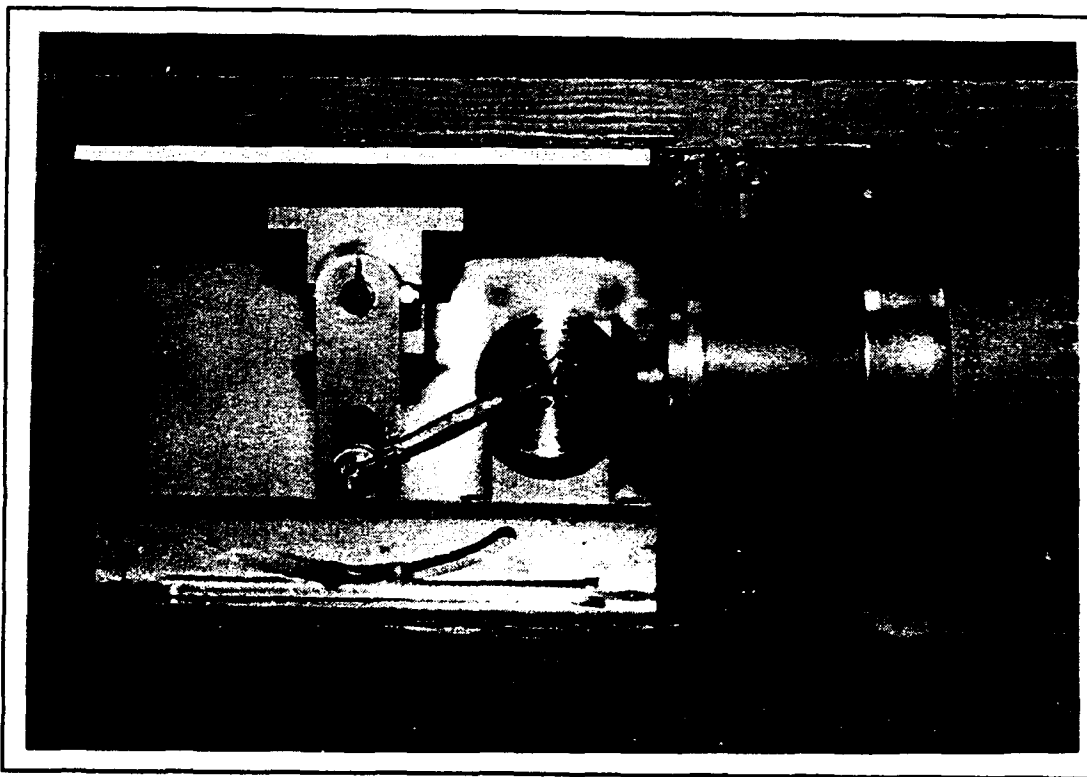


Figure A4: Canard Oscillation-Mechanism

mechanism can be seen in Figure A4. The redesign allowed for changes to the mean deflection angle, amplitude and frequency of the canard oscillation. The mean deflection angle was set by adjusting the turnbuckle attached to the canard shaft-arm and the eccentric-hub. The amplitude was adjusted by changing the hole in which the turnbuckle was connected in the eccentric-hub, and fine adjustments were made by sliding the turnbuckle up or down in the canard shaft-arm. Frequency was controlled by the motor and a variable power supply. The pivot-point for the canard was moved from 7% MAC (40% exposed root chord) to 25% MAC to reduce changes in pitching-moment with changes in deflection angle and thus reduce the loading on the oscillation mechanism. Also, past work has involved dynamic-stall configurations pivoted about 25% MAC; this modification would put the current study in line with previous efforts. This change moved the canard forward on the model and changed the basic configuration determined to be optimal by Lacey [Ref. 5] with x/c less than or equal to 1.5, where x is the distance from 40% of the canard exposed root chord to 25% MAC of the wing and c is the MAC of the main wing as determined by Equation A3.

$$MAC = \frac{2}{3} (C_r + C_t - \frac{C_r C_t}{C_r + C_t}) \quad (A3)$$

To compensate for the new configuration, a new wing was designed.

C. WING MODIFICATIONS

The wing maintained the same basic dimensions as the wing used by Schmidt [Ref. 12], with a leading-edge sweep equal to 50° , taper ratio (λ) equal to 0.15 and an aspect ratio (AR) equal to 3, but the overall size was changed from 68.89 square inches to 90.19 square inches (exposed area) as seen in Figure A5. This larger main wing resulted in an x/c equal to 1.44 which was within parameters as specified by Lacey [Ref. 5]. Additionally, previous research done by Lacey [Ref. 5], Kersh [Ref. 11] and Schmidt [Ref. 12] used main-wing areas to the fuselage centerline. Because the fuselage is very large in order to house the canard-oscillation mechanism, distorted area ratios resulted because the bulk of the projected wing-area was inside the fuselage. Therefore, the exposed wing-area was used when sizing the airfoil and resulted in a ratio of the canard exposed-area to the wing exposed-area (S_{ce}/S_{we}) of 0.21. The vertical separation between the canard and wing, z/c , was equal to 0.21 where z was the vertical distance between the main wing and the canard. This parameter is within the optimum range for z/c of 0.1 to 0.25 as determined by Lacey [Ref. 5].

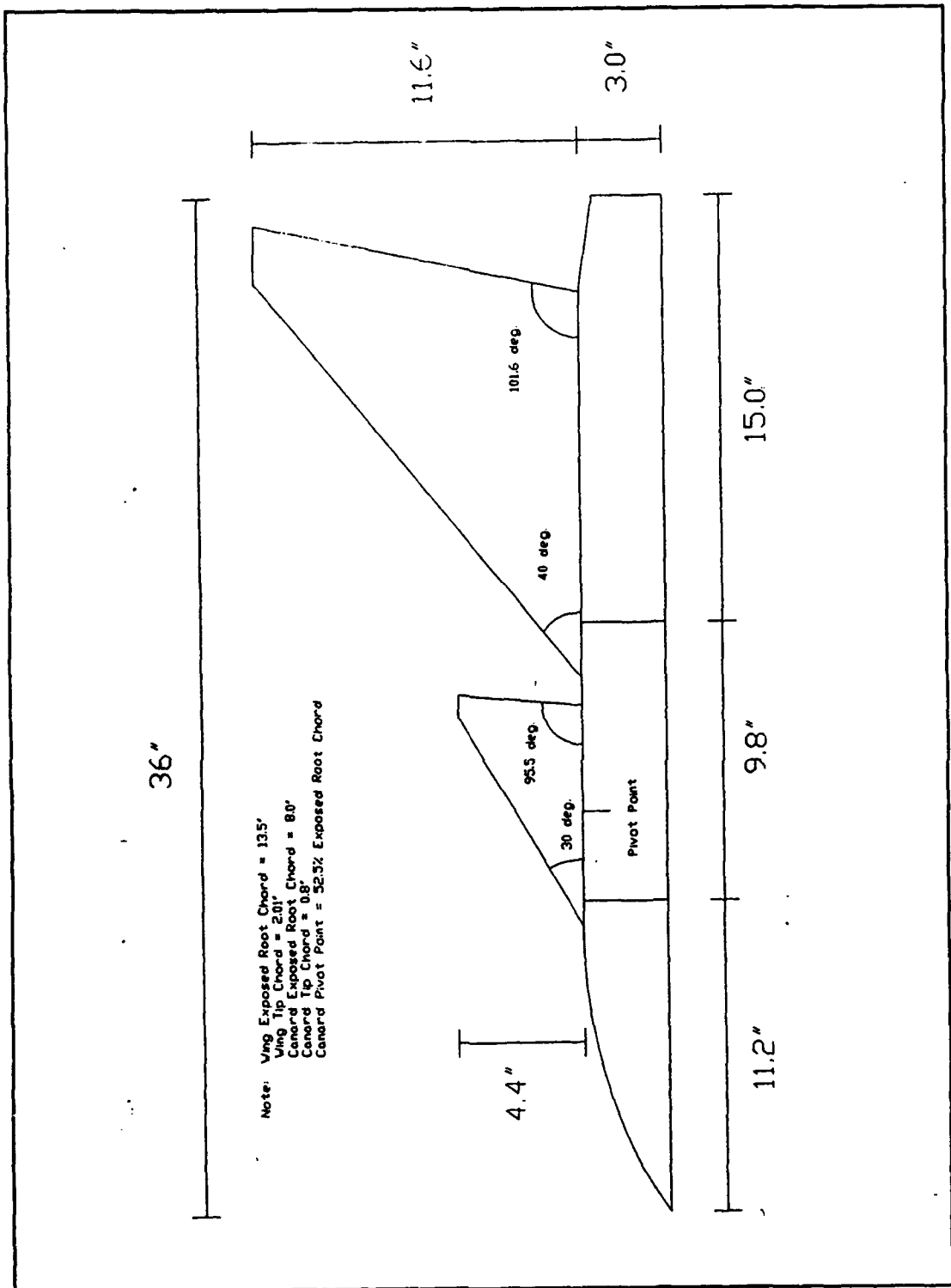


Figure A5: Model Configuration

APPENDIX B: BALANCE CALIBRATION

Procedures as outlined in Schmidt [Ref. 12] were utilized to obtain the calibration matrix to be utilized in the data acquisition program (see Data Acquisition, Appendix C). Additionally, it was sought to duplicate the calibration operation and to obtain a similar calibration matrix, thus validating the results obtained by Schmidt [Ref. 12].

An externally-mounted cylindrical-type balance with strain-gages located at the base (pair A) and the top (pair B) of the balance has been discussed previously. Strain-gage pair A and B were separated by a vertical distance of 26.5 inches and temperature compensation was accomplished utilizing four active legs for each strain-gage bridge. A schematic of the balance and strain gage location can be seen in Figure B1. The top of the balance or turntable was flush with the reflection-plane in the test-section of the low-speed wind tunnel and a calibration rig was mounted to the turntable for the calibration process as shown in Figure B1. With the Pacific^o 8255 operational amplifiers set to a gain of 1000, and the MC-MIO-16L-9 board set to a gain of 1, the system was capable of analog-to-digital conversion with a 4.88-mvolt resolution. With the calibration rig installed, the angle-of-attack readout at the base of the balance was visually set to ensure that the angle of attack read on the base corresponded to the actual model angle of attack. The inputs to the

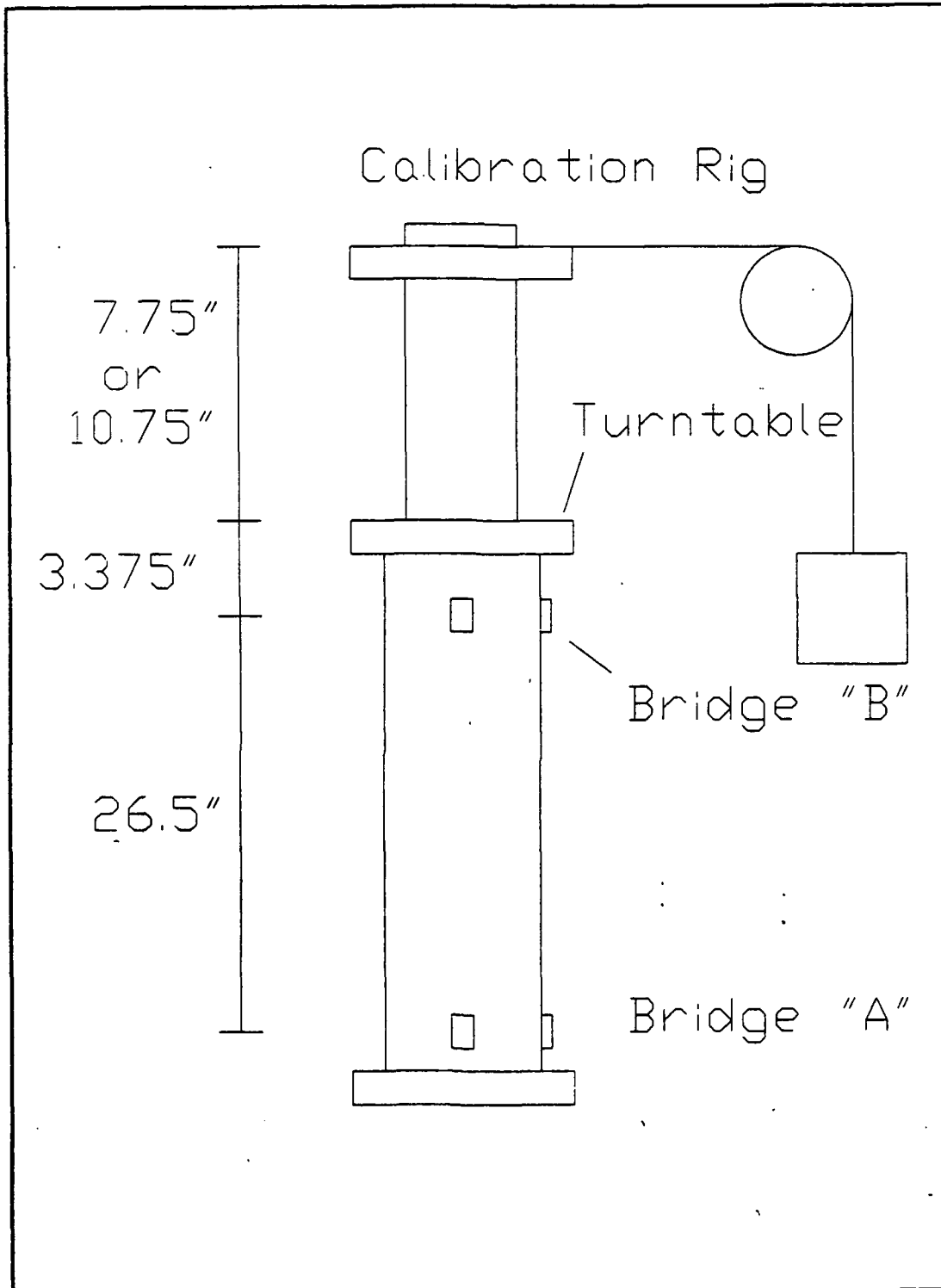


Figure B1: Strain-Gage Balance Schematic

operational amplifiers were shorted and the gain set to 1; the amplifier output was then adjusted to $0.0 \pm 100.0 \mu\text{volts}$. The gain was then set to 1000 and the amplifier input was adjusted to $0.0 \pm 500.0 \mu\text{volts}$. The shorts were removed and the signal conditioners were set to a span voltage of $10 \pm 0.05 \text{ volts}$ and the span zeroes were set to $0.0 \pm 0.05 \text{ volts}$.

Because the balance was only capable of rotation from -18° to $+200^\circ$, and the installation of the model required the turntable to rotate from 0° to -90° , the turntable was rotated 90° so that a 90° reading on the turntable base (see Figure B2) corresponded to a model angle of attack equal to 0° . Because of this rotation, the normal and axial force measurements were rotated 90° as seen in Figure B3. The data acquisition and force reduction equations accounted for this offset where the 90° position corresponded to the 0° position in the new coordinate system. The nomenclature for each strain-gage is as follows:

Eaa - Voltage at the lower axial-force bridge.

Eba - Voltage at the upper axial-force bridge.

Ean - Voltage at the lower normal-force bridge.

Ebn - Voltage at the upper normal-force bridge.

(a - b) - Height above turntable of first cable attachment ($h=10.75 \text{ in.}$).

(a' - b) - Height above turntable of second cable attachment ($h=7.75 \text{ in.}$).

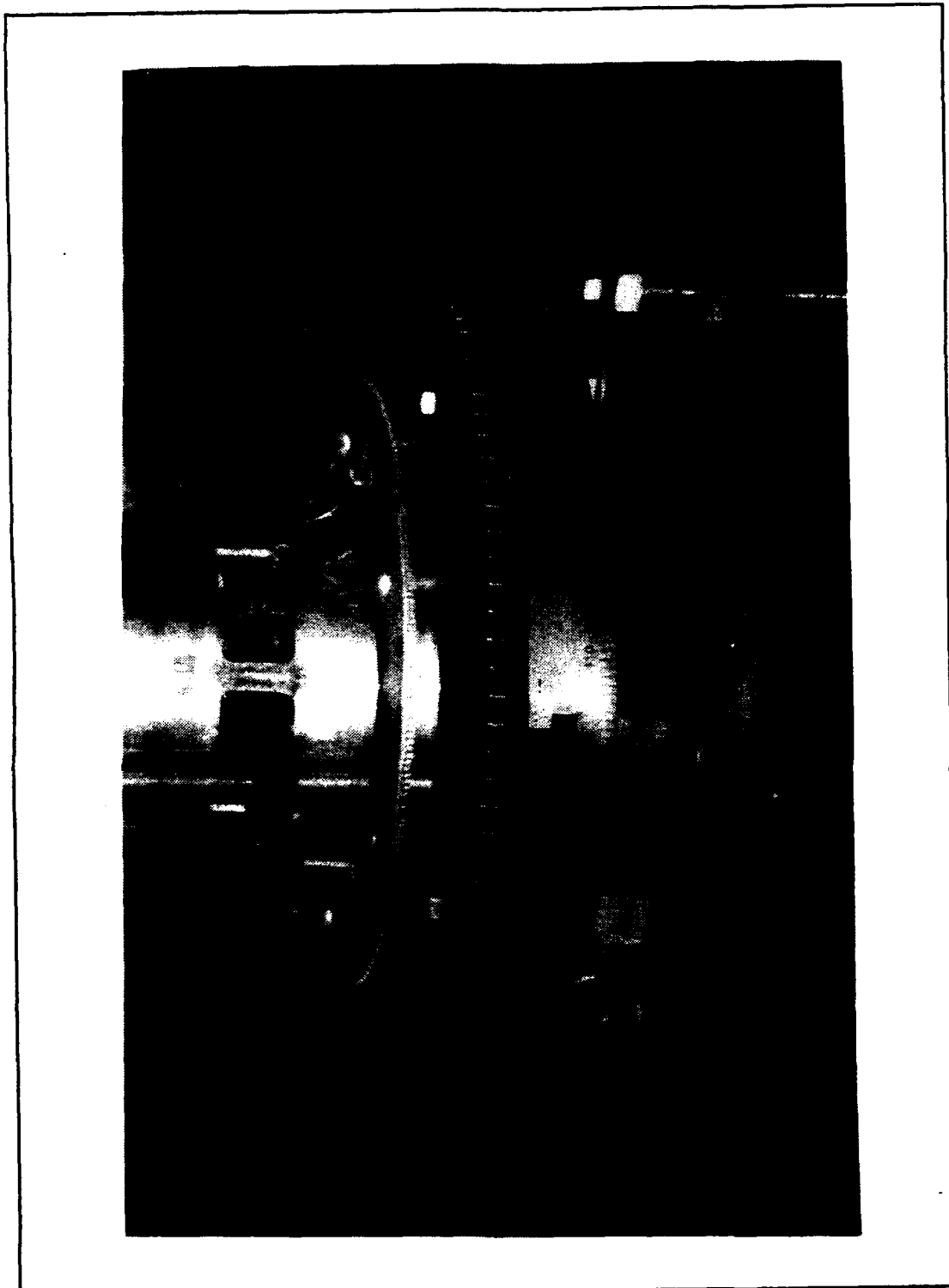
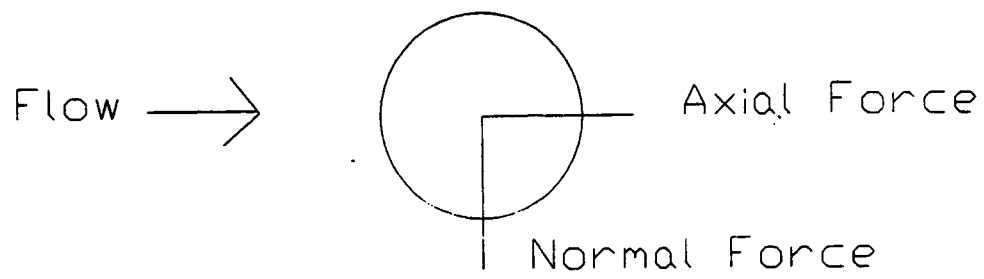


Figure B2: Balance Base and Markings

Turntable at "0" degrees



Turntable at "90" degrees

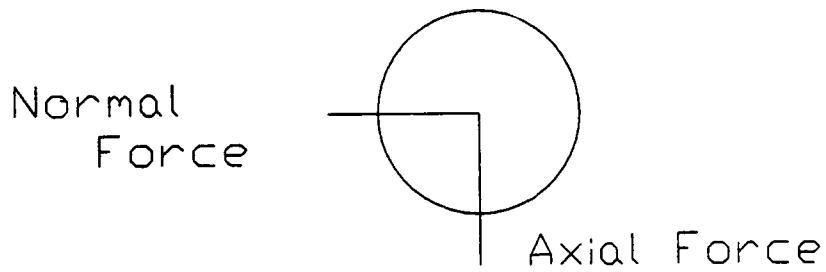


Figure B3: Coordinate System Change

The calibration procedure consisted of rotating the turntable to either 0° or 90° , as measured in the new coordinate system, and suspending increasing increments of



Figure B4: Calibration Rig and Pulley

weights on the calibration rig (see Figure B4 and B5) at two heights above the turntable and using the data acquisition system to record the voltage readings obtained. The cable height was measured vertically from the reflection plane to the cable and a sight-level was used to ensure the cable was horizontal.

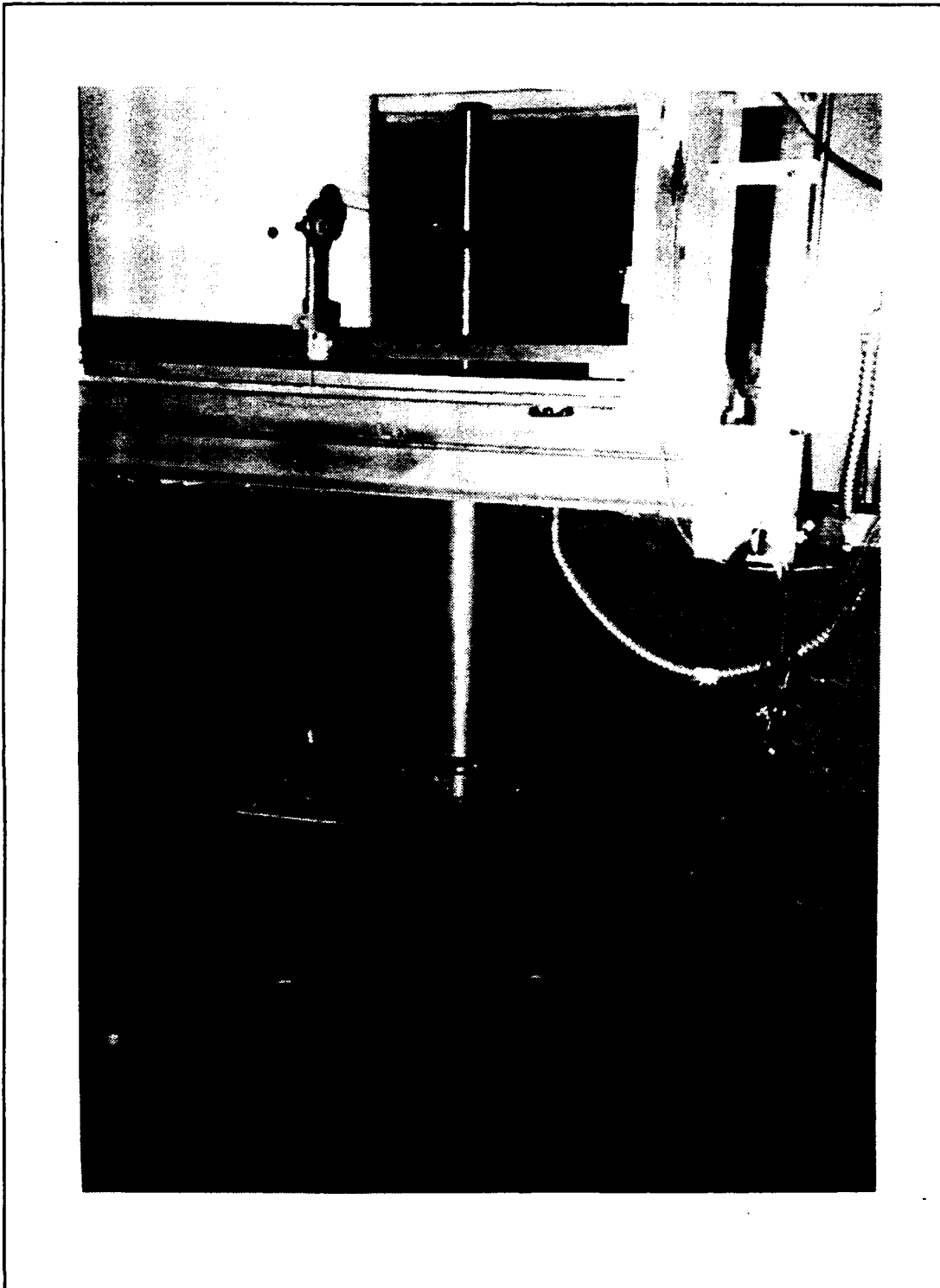


Figure B5: Calibration Rig and Weight Cage

Equation B1 is the basic equation used to determine the calibration-matrix:

$$[K] \begin{bmatrix} d\Delta E \\ dLOAD \end{bmatrix} = \begin{bmatrix} \begin{bmatrix} FORCES \\ FORCES \end{bmatrix} & [0] \\ \begin{bmatrix} FORCES \\ MOMENTS \end{bmatrix} & [0] \\ [0] & \begin{bmatrix} FORCES \\ FORCES \end{bmatrix} \\ [0] & \begin{bmatrix} FORCES \\ MOMENTS \end{bmatrix} \end{bmatrix} \quad (B1)$$

where [K] and [dΔ/dLOAD] are 4 X 4 matrices. The 1 X 2 sub-matrices on the right hand side are for moment resolution and the entire equation can be expanded as follows:

$$\begin{bmatrix} K_{11} & K_{12} & K_{13} & K_{14} \\ K_{21} & K_{22} & K_{23} & K_{24} \\ K_{31} & K_{32} & K_{33} & K_{34} \\ K_{41} & K_{42} & K_{43} & K_{44} \end{bmatrix} \begin{bmatrix} \frac{d\Delta E_{aa}}{dA} & \frac{d\Delta E'_{aa}}{dA} & \frac{d\Delta E_{aa}}{dN} & \frac{d\Delta E'_{aa}}{dN} \\ \frac{d\Delta E_{ba}}{dA} & \frac{d\Delta E'_{ba}}{dA} & \frac{d\Delta E_{ba}}{dN} & \frac{d\Delta E'_{ba}}{dN} \\ \frac{d\Delta E_{an}}{dA} & \frac{d\Delta E'_{an}}{dA} & \frac{d\Delta E_{an}}{dN} & \frac{d\Delta E'_{an}}{dN} \\ \frac{d\Delta E_{bn}}{dA} & \frac{d\Delta E'_{bn}}{dA} & \frac{d\Delta E_{bn}}{dN} & \frac{d\Delta E'_{bn}}{dN} \end{bmatrix} = \begin{bmatrix} 1 & 1 & 0 & 0 \\ (a-b) & (a'-b) & 0 & 0 \\ 0 & 0 & 1 & 1 \\ 0 & 0 & (a-b) & (a'-b) \end{bmatrix} \quad (B2)$$

The right side of the equation is known with (a-b) equal to 7.75 inches and (a'-b) equal to 10.75 inches. The slopes of the voltage readings with respect to load, cable height and turntable angle of attack (0°, 90°) were determined using the calibration data and performing a linear-regression analysis to fill in the slope matrix ([dΔE/dLOAD]). Both sides of the Equation B2 were pre-multiplied by the inverse of the slope matrix resulting in the determination of the calibration matrix [K]. The response of the strain-gages were linear within the load ranges tested and graphical results of the calibration process can be seen in Figures B6 through B9.

The normal and axial forces as well as the normal and axial moments were resolved using Equation B3:

$$\begin{bmatrix} A_f \\ a_m \\ N_f \\ n_m \end{bmatrix} = [K] \begin{bmatrix} E_{aa} \\ E_{ba} \\ E_{an} \\ E_{bn} \end{bmatrix} \quad (B3)$$

where:

A_f = Axial force (lbf)

a_m = Axial moment (ft lbf)

N_f = Normal force (lbf)

n_m = Normal moment (ft lbf)

[K] = Calibration-matrix

E_{aa} (etc.) = Strain-gage voltage output

Lift and drag were calculated using Equations B4 and B5:

$$L = A_f \cos(\alpha) + N_f \sin(\alpha) \quad (B4)$$

$$D = A_f \sin(\alpha) - N_f \cos(\alpha) \quad (B5)$$

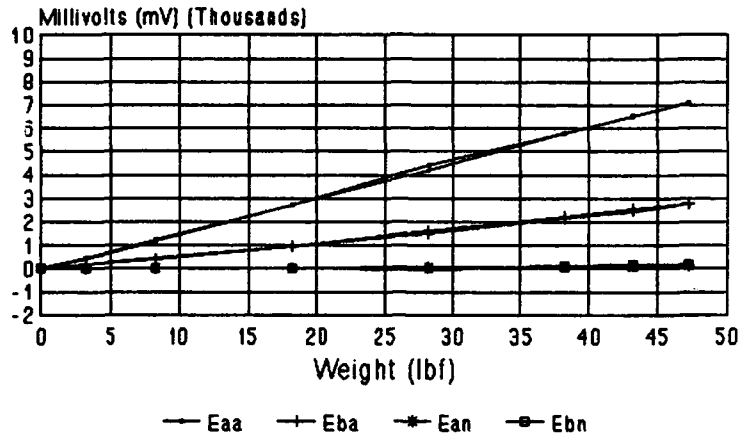
where:

α = model angle of attack

and all other variables were previously defined in Equation B3. The results were recorded to floppy disc.

The non-dimensional axial and normal coefficients were calculated using equations similar to Equations 2 and 3 in Chapter IV.

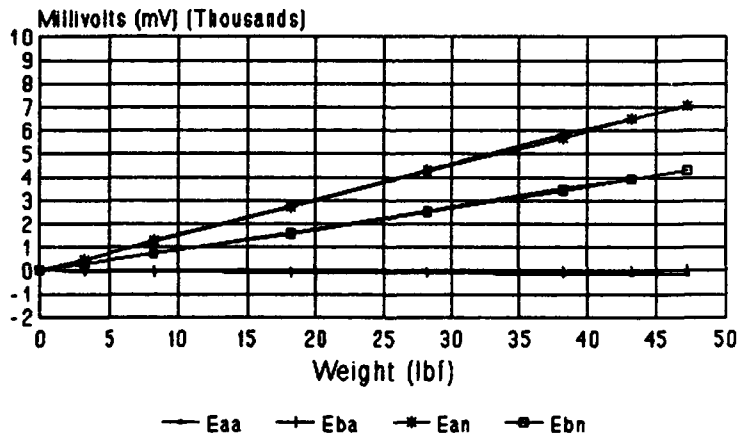
Axial Voltage Readings Average Calibration Data



h = 7.75 in.

Figure B6: Axial Calibration Data

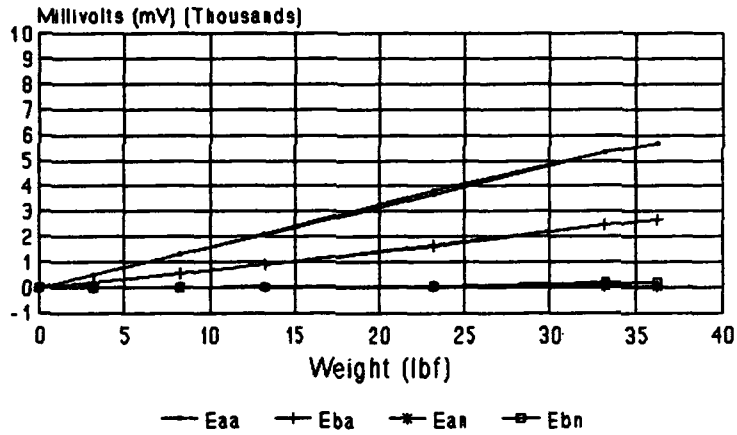
Normal Voltage Readings Average Calibration Data



h = 7.75 in.

Figure B7: Normal Calibration Data

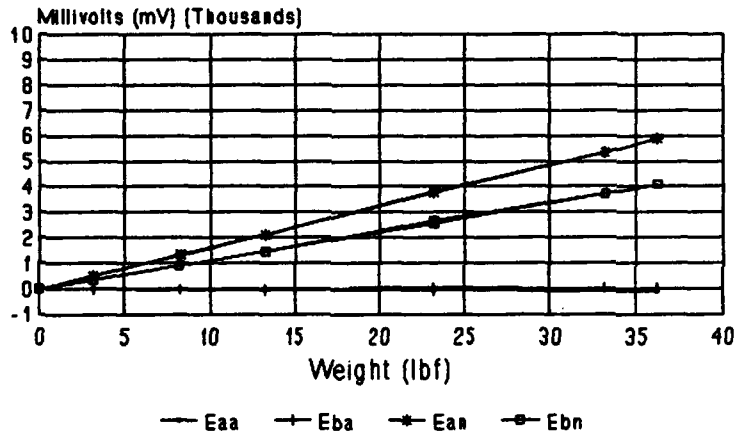
Axial Voltage Readings Average Calibration Data



h = 10.75 in.

Figure B8: Axial Calibration Data

Normal Voltage Readings Average Calibration Data



h = 10.75 in.

Figure B9: Normal Calibration Data

REDUCED CALIBRATION DATA

AXIAL VOLTAGE READINGS WITH CABLE HEIGHT = 10.75 in.

weight	Eaa	Eba	Ean	Ebn
0	0.002442	0.200196	0.50293	0.313721
3.204	488.3191	196.5137	5.997314	4.641113
8.21	1298.835	535.1221	12.44751	10.61401
13.206	2074.525	876.8555	21.7395	24.01978
23.209	3673.109	1598.728	32.00317	54.35669
33.213	5339.808	2454	42.54395	168.8855
36.217	5703.39	2650.382	46.03272	199.7754
33.213	5328.344	2468.192	42.15332	184.7668
23.209	3834.091	1675.983	36.04126	57.15942
13.206	2110.815	894.7705	21.92627	22.13501
8.21	1291.871	533.2349	12.18994	11.13892
3.204	500.1721	203.2727	6.73584	4.321289
0	0.643311	-0.16602	-0.09644	0.067139

REDUCED CALIBRATION DATA

AXIAL VOLTAGE READINGS WITH CABLE HEIGHT = 7.75 in.

weight	Eaa	Eba	Ean	Ebn
0	0.042725	0.230713	0.283203	0.437012
3.204	433.8098	160.3003	8.164063	0.26001
8.21	1170.98	415.7166	21.18897	0.598145
18.212	2689.73	950.6494	44.15039	-3.47778
28.215	4210.483	1488.39	66.30127	-5.23682
38.219	5807.573	2141.951	87.79785	61.61865
43.229	6489.89	2460.868	95.65674	119.4885
47.236	7098.215	2759.36	106.6199	183.6609
43.229	6528.105	2536.877	100.6201	174.9036
38.219	5788.529	2205.037	91.33179	122.9675
28.215	4422.993	1618.656	72.67822	47.44263
18.212	2709.492	980.3992	48.10181	28.1543
8.21	1243.868	441.5149	23.85742	11.10352
3.204	458.8501	163.6304	9.554443	4.394531
0	0	-0.05615	0.009766	0.037842

REDUCED CALIBRATION DATA

NORMAL VOLTAGE READINGS WITH CABLE HEIGHT = 10.75 in.

weight	Eaa	Eba	Ean	Ebn
0	-0.0354	-0.04639	0.252685	0.45166
3.204	-6.35742	-15.2698	508.6426	342.2449
8.21	-18.2312	-33.2935	1339.437	900.6689
13.206	-29.1589	-28.2129	2116.339	1441.707
23.209	-52.865	31.71997	3804.698	2682.972
33.213	-73.8831	16.37329	5319.387	3721.821
36.217	-83.1555	7.347412	5872.511	4095.486
33.213	-76.9397	8.337403	5331.328	3717.717
23.209	-54.6875	-44.6008	3750.99	2579.695
13.206	-30.8728	-53.4937	2105.709	1430.215
8.21	-19.1748	-35.1257	1297.524	877.9834
3.204	-7.03491	-13.6133	511.5002	345.2881
0	-0.03784	0.062256	0.05127	-0.14648

REDUCED CALIBRATION DATA

NORMAL VOLTAGE READINGS WITH CABLE HEIGHT = 7.75 in.

weight	Eaa	Eba	Ean	Ebn
0	-0.08179	0.146485	-0.24536	0.039062
3.204	-10.1282	-12.3987	475.0464	276.8579
8.21	-27.5647	-37.3169	1223.66	711.1499
18.212	-62.0129	-69.071	2687.106	1570.194
28.215	-99.5422	-62.6099	4225.94	2509.735
38.219	-134.57	-14.4495	5684.46	3433.84
43.229	-153.827	-11.1719	6529.763	3948.425
47.236	-165.776	44.88281	7072.443	4319.435
43.229	-152.38	-23.4387	6509.513	3926.559
38.219	-136.27	-44.5374	5851.049	3511.797
28.215	-102.057	-69.3469	4316.512	2562.994
18.212	-63.7305	-73.8782	2767.905	1625.876
8.21	-28.5706	-37.1631	1266.998	740.8362
3.204	-9.98535	-13.5437	464.7095	272.749
0	0.024414	0.2771	0.050049	0.91919

APPENDIX C: DATA ACQUISITION PROGRAM

This program was written and compiled using LabWindows and QuickBasic 4.5. (used "bc /o multi" to compile) Its purpose is to read and convert voltages from four channels connected to the strain gauges on the Academic wind tunnel. The voltages are converted to normal and axial forces and moments with respect to the balance. It was written and modified by LT Tom D. Stuart and LT Dean C. Schmidt, 20 June 92. It was further modified by LT Douglas G. Mc Bane on 12 January 1993. It follows the nomenclature used by Kersh where the table is rotated 90 degrees and the axial force is normal to the flow direction and the normal force is parallel to the flow direction (opposite direction). However, the lift and drag components are converted so that the lift is perpendicular to the flow direction and the drag is parallel to the flow direction (same direction) concurrent with standard notation.

' Variables explained

' eaa = Strain gauge voltage at point A in Axial direction.
' eba = Strain gauge voltage at point B in Axial direction.
' ean = Strain gauge voltage at point A in Normal direction.
' ebn = Strain gauge voltage at point B in Normal direction.

' AX = Axial force
' Max = Axial moment
' NORM = Normal force
' Mnorm = Normal moment

' alpha = Angle of Attack of the model
' LIFT = Lift force
' DRAG = Drag force

'*****

```
REM $INCLUDE: 'C:\LW\INCLUDE\LWSYSTEM.INC'  
REM $INCLUDE: 'C:\LW\INCLUDE\GPIB.INC'  
REM $INCLUDE: 'C:\LW\INCLUDE\FORMATIO.INC'  
REM $INCLUDE: 'C:\LW\INCLUDE\GRAPHICS.INC'  
REM $INCLUDE: 'C:\LW\INCLUDE\ANALYSIS.INC'  
REM $INCLUDE: 'C:\LW\INCLUDE\DATAACQ.INC'  
REM $INCLUDE: 'C:\LW\INCLUDE\RS232.INC'
```

```
DIM K$(4,4)  
DIM ean.array$(1000), eaa.array$(1000), ebn.array$(1000),  
    eba.array$(1000)
```

C O M M O N S H A R E D
ean.array#(), eaa.array#(), ebn.array#(), eba.array#()

DECLARE SUB volt (ean#, eaa#, ebn#, eba#, alpha#)
DECLARE SUB aero (AX#, NORM#, LIFT#, DRAG#, alpha#)
D E C L A R E S U B f o r c e s
(K#(), eaa#, eba#, ean#, ebn#, AX#, Max#, NORM#, Mnorm#, alpha#)

SCREEN 9, 0
COLOR 15, 1

ea0# = 0
eaa0# = 0
ean0# = 0
ebn0# = 0

' CALIBRATION MATRIX INPUT (See thesis for explanation)

DATA 0.009292, -0.007686, -0.000053, -0.000209
DATA -0.033079, 0.246045, 0.007737, 0.003644
DATA 0.000063, -0.000417, 0.009682, -0.004241
DATA 0.002432, -0.006519, -0.033848, 0.126897

FOR L% = 1 TO 4: FOR M% = 1 TO 4
READ K#(L%, M%) : NEXT M%
NEXT L%

LOCATE 10, 20: INPUT "Type the name of the voltage output
file"; VOL\$
VOL\$ = "C:\LW\INSTR\DOUG\" + VOL\$ + ".DAT"
OPEN VOL\$ FOR APPEND AS #1

CLS: LOCATE 10, 20: INPUT "Type the name of the forces output
file"; FM\$
FM\$ = "C:\LW\INSTR\DOUG\" + FM\$ + ".DAT"
OPEN FM\$ FOR APPEND AS #2

CLS: LOCATE 10, 20: INPUT "TYPE THE NAME OF LIFT/DRAG FILE";
LD\$
LD\$ = "C:\LW\INSTR\DOUG\" + LD\$ + ".DAT"
OPEN LD\$ FOR APPEND AS #3

500

'ALPHA! IS AOA READ OFF HUB OF TURNTABLE
'ALPHA# IS AOA OF MODEL WRT AIRFLOW

```

CLS: LOCATE 10, 20: INPUT "Input the Test AOA (deg.)"; alpha!
ALPHA#=90 - ALPHA!
'*****
'CANARD INCIDENCE IS WRT TO FUSELAGE CENTERLINE
'*****

LOCATE 15, 20: INPUT "Input canard incidence (deg.)"; CANARD#

LOCATE 20, 20: INPUT "Input oscillation frequency (Hz)"; HZ#

CLS: LOCATE 5, 20: INPUT "Is this a tare (zero load) reading?
(Y/N)"; A$

IF A$ = "Y" THEN CALL tare (ean0#, eaa0#, ebn0#, eba0#, alpha#)

LOCATE 23,15: INPUT "Ready to take readings? (Y/N)"; B$

IF B$ = "Y" THEN CALL volt (ean#, eaa#, ebn#, eba#, alpha#)
IF B$ <> "Y" THEN GOTO 5000

' Correcting for zero load values.

eaa# = eaa# - eaa0#
eba# = eba# - eba0#
ean# = ean# - ean0#
ebn# = ebn# - ebn0#

C      A      L      L      f      o      r      c      e      s
(K#( ), eaa#, eba#, ean#, ebn#, AX#, Max#, NORM#, Mnorm#, alpha#)

CALL aero (AX#, NORM#, LIFT#, DRAG#, alpha#)

PRINT " "
PRINT " AOA      EAA (mV)      EBA (mV)      EAN (mV)      EBN(mV)"
PRINT " ***      *****      *****      *****      *****"

PRINT USING " ###.####"; alpha#; eaa#; eba#; ean#; ebn#
PRINT #1, USING "###.####"; alpha#; eaa#; eba#; ean#; ebn#

PRINT " "
PRINT " AXIAL (lb) MOMax (ft-lb) NORMAL (lb) MOMnorm(ft-lb)"
PRINT " ***** ***** ***** *****"

PRINT USING " ###.####"; AX#; Max#; NORM#; Mnorm#
PRINT #2, USING "###.####"; alpha#; AX#; NORM#; LIFT#; DRAG#

PRINT " "
PRINT " Lift (lb) Drag (lb) CANARD (AOA) CANARD FREQ(HZ)"
PRINT " ***** ***** ***** *****"

```

```
PRINT USING "    ###.####"; LIFT#; DRAG#; CANARD#; HZ#
PRINT #3, USING "###.####"; LIFT#; DRAG#; CANARD#; HZ#;
ALPHA#
```

```
LOCATE 23, 15: INPUT "Do you want another reading? (Y/N)";
ANS$
IF ANS$ = "Y" THEN GOTO 500
```

```
5000 CLOSE #1
CLOSE #2
CLOSE #3
```

```
END
```

```
'*****
'END OF MAIN PROGRAM.  SUBROUTINES START FROM HERE
'*****
'*****
'*****
SUB volt (ean#, eaa#, ebn#, eba#, alpha#)
'*****
' S/R to read Channel 0,2,4,6 on MIO-16L-9 for Analog Voltage
,
'*****

' Setting Board code for MIO-16L-9

board.code%=0

'*****

err1.num% = Init.DA.Brds(1, board.code%)

err2.num% = AI.Setup(1, 0, 1)
err3.num% = AI.Setup(1, 2, 1)
err4.num% = AI.Setup(1, 4, 1)
err5.num% = AI.Setup(1, 6, 1)

' Configure and set clock to 1MHZ

err6.num% = CTR.Clock (1, 1, 1, 1)
err7.num% = CTR.Config (1, 1, 0, 0, 0, 0)

LWtotal! = 0

FOR i% = 1 TO 1000

err8.num% = CTR.EvCount (1, 1, 1, 0)
```

```

' CH 0 = Eaa
  err9.num% = AI.Read(1, 0, 1, value0%)
  er10.num% = AI.Scale(1, 1, value0%, eaa.array#(i%))

' CH 2 = Eba
  er11.num% = AI.Read(1, 2, 1, value2%)
  er12.num% = AI.Scale(1, 1, value2%, eba.array#(i%))

' CH 4 = Ean
  er13.num% = AI.Read(1, 4, 1, value4%)
  er14.num% = AI.Scale(1, 1, value4%, ean.array#(i%))

' CH 6 = Ebn
  er15.num% = AI.Read(1, 6, 1, value6%)
  er16.num% = AI.Scale(1, 1, value6%, ebn.array#(i%))

er17.num% = CTR.EvRead (1, 1, overflo%, tcount%)

LWtotal! = LWtotal! + tcount%

NEXT i%

CLS:LOCATE 5,15:PRINT "Total Time is " LWtotal!*1E-6"
seconds."

CALL Mean (eaa.array#(), 1000, eaa#)
CALL Mean (eba.array#(), 1000, eba#)
CALL Mean (ean.array#(), 1000, ean#)
CALL Mean (ebn.array#(), 1000, ebn#)

'*****
' This multiplication (*1000) will make the voltages in mV

eaa#=eaa#*1000
eba#=eba#*1000
ean#=ean#*1000
ebn#=ebn#*1000

END SUB

'*****
'*****

S      U      B      f      o      r      c      e      S
(K#(), eaa#, eba#, ean#, ebn#, AX#, Max#, NORM#, Mnorm#, alpha#)

```

' FORCES AND MOMENTS CALCULATIONS (See thesis for explanation)

AX# = K#(1,1)*eaa# +K#(1,2)*eba# +K#(1,3)*ean# +K#(1,4)*ebn#
Max# = K#(2,1)*eaa# +K#(2,2)*eba# +K#(2,3)*ean# +K#(2,4)*ebn#
NORM# = K#(3,1)*eaa# +K#(3,2)*eba# +K#(3,3)*ean# +K#(3,4)*ebn#
Mnorm# = K#(4,1)*eaa#+K#(4,2)*eba# +K#(4,3)*ean# +K#(4,4)*ebn#

END SUB

' *****
' *****

SUB aero (AX#,NORM#,LIFT#,DRAG#,alpha#)

' *****

PI# = 3.14159265359

LIFT# = AX#*COS(PI#/180*alpha#) + NORM#*SIN(PI#/180*alpha#)

DRAG# = AX#*SIN(PI#/180*alpha#) - NORM#*COS(PI#/180*alpha#)

END SUB

' *****
' *****

SUB tare (ean#,eaa#,ebn#,eba#,alpha#)

' *****

'

' S/R to read Channel 0,2,4,6 on MIO-16L-9 for Analog Voltage

'

' *****

' Setting Board code for MIO-16L-9

board.code%=0

' *****

CLS: LOCATE 5, 20: INPUT "Ready to take tare readings? (Y/N)";
T\$

IF T\$ <> "Y" THEN RETURN

err1.num% = Init.DA.Brds(1, board.codr%)

err2.num% = AI.Setup(1, 0, 1)

err3.num% = AI.Setup(1, 2, 1)

err4.num% = AI.Setup(1, 4, 1)

```

err5.num% = AI.Setup(1, 6, 1)

' Configure and set clock to 1MHZ

err6.num% = CTR.Clock (1, 1, 1, 1)
err7.num% = CTR.Config (1, 1, 0, 0, 0, 0)

LWtotal! = 0

FOR i% = 1 TO 1000

err8.num% = CTR.EvCount (1, 1, 1, 0)

' CH 0 = Eaa
  err9.num% = AI.Read(1, 0, 1, value0%)
  er10.num% = AI.Scale(1, 1, value0%, eaa.array#(i%))

' CH 2 = Eba
  er11.num% = AI.Read(1, 2, 1, value2%)
  er12.num% = AI.Scale(1, 1, value2%, eba.array#(i%))

' CH 4 = Ean
  er13.num% = AI.Read(1, 4, 1, value4%)
  er14.num% = AI.Scale(1, 1, value4%, ean.array#(i%))

' CH 6 = Ebn
  er15.num% = AI.Read(1, 6, 1, value6%)
  er16.num% = AI.Scale(1, 1, value6%, ebn.array#(i%))

er17.num% = CTR.EvRead (1, 1, overflo%, tcount%)

LWtotal! = LWtotal! + tcount%

NEXT i%

CLS:LOCATE 5,15:PRINT "Total Time is " LWtotal!*1E-6"
seconds."

CALL Mean (eaa.array#(), 1000, eaa#)
CALL Mean (eba.array#(), 1000, eba#)
CALL Mean (ean.array#(), 1000, ean#)
CALL Mean (ebn.array#(), 1000, ebn#)

'*****

' This multiplication (*1000) will make the voltages in mV

eaa#=eaa#*1000
eba#=eba#*1000

```

```
ean#=ean#*1000
ebn#=ebn#*1000
```

```
PRINT " "
PRINT " AOA      EAA (mV)      EBA (mV)      EAN (mV)      EBN (mV) "
PRINT " ***      *****      *****      *****      *****"
```

```
PRINT USING "    ###.#####"; alpha#; eaa#; eba#; ean#; ebn#
PRINT #1, USING "###.#####"; alpha#; eaa#; eba#; ean#; ebn#
```

```
END SUB
```

APPENDIX D: EXPERIMENTAL DATA

MODEL AOA=	22					
CANARD AOA=	4					
AMPLITUDE=	5					
DELTA P (cm. H2O)=	12					
q (lb/ft ²)=	27.33					
S (ft ²)=	0.9383					
MAC (in.)=	5.38					
VELOCITY (ft/s)=	151.6454					
FREQUENCY						
Hz=	0	5	10	15	20	25
k=	0	0.046439	0.092877	0.139316	0.185754	0.232193
LIFT						
MEAN LIFT =	36.88612	36.6991	36.63613	36.51826	36.39341	36.18825
STD. DEV.=	0.095674	0.076712	0.06343	0.087532	0.071285	0.074271
3.182*STD.DEV.=	0.304434	0.244098	0.201833	0.278528	0.22683	0.236331
UPPER LIMIT=	37.19056	36.94319	36.83797	36.79679	36.62024	36.42458
LOWER LIMIT=	36.58169	36.455	36.4343	36.23973	36.16658	35.95192
MEAN Cl =	1.438407	1.431113	1.428658	1.424061	1.419193	1.411192
Cl STD.DEV.=	0.003731	0.002991	0.002473	0.003413	0.00278	0.002896
3.182*STD.DEV.=	0.011872	0.009519	0.007871	0.010861	0.008845	0.009216
UPPER LIMIT=	1.450278	1.440632	1.436529	1.434923	1.428038	1.420408
LOWER LIMIT=	1.426535	1.421595	1.420787	1.4132	1.410347	1.401977
DRAG						
MEAN DRAG =	14.80508	14.62032	14.56883	14.5075	14.46842	14.30809
STD. DEV.=	0.036154	0.041282	0.027567	0.03825	0.021701	0.032489
3.182*STD.DEV.=	0.115043	0.13136	0.087718	0.121712	0.069052	0.10338
UPPER LIMIT=	14.92012	14.75168	14.65654	14.62922	14.53747	14.41147
LOWER LIMIT=	14.69003	14.48896	14.48111	14.38579	14.39937	14.20471
MEAN Cd =	0.577337	0.570132	0.568124	0.565733	0.564209	0.557957
Cd STD.DEV.=	0.00141	0.00161	0.001075	0.001492	0.000846	0.001267
3.182*STD.DEV.=	0.004486	0.005122	0.003421	0.004746	0.002693	0.004031
UPPER LIMIT=	0.581823	0.575255	0.571545	0.570479	0.566902	0.561988
LOWER LIMIT=	0.572851	0.56501	0.564703	0.560987	0.561516	0.553925

MODEL AOA=	22					
CANARD AOA=	7					
AMPLITUDE=	5					
DELTA P (cm. H2O)=	12					
q (lbf/ft^2)=	27.33					
S (ft^2)=	0.9383					
MAC (in.)=	5.38					
VELOCITY (ft/s)=	151.6454					
FREQUENCY						
Hz=	0	5	10	15	20	25
k=	0	0.046439	0.092877	0.139316	0.185754	0.232193
LIFT						
MEAN LIFT =	36.73228	37.22737	37.24034	37.12729	36.95755	36.80912
STD. DEV.=	0.108599	0.095732	0.045358	0.079247	0.087175	0.06417
3.182*STD.DEV.=	0.345563	0.304621	0.144331	0.252165	0.27739	0.204187
UPPER LIMIT=	37.07784	37.53199	37.38467	37.37945	37.23494	37.01331
LOWER LIMIT=	36.38672	36.92275	37.09601	36.87512	36.68016	36.60493
MEAN Cl =	1.432407	1.451714	1.45222	1.447811	1.441192	1.435404
Cl STD.DEV.=	0.004235	0.003733	0.001769	0.00309	0.003399	0.002502
3.182*STD.DEV.=	0.013476	0.011879	0.005628	0.009833	0.010817	0.007962
UPPER LIMIT=	1.445883	1.463593	1.457848	1.457644	1.452009	1.443366
LOWER LIMIT=	1.418932	1.439835	1.446591	1.437978	1.430375	1.427441
DRAG						
MEAN DRAG =	15.29447	13.97594	13.95861	13.93514	13.8817	13.83226
STD. DEV.=	0.045459	0.04185	0.019704	0.029195	0.031175	0.01424
3.182*STD.DEV.=	0.14465	0.133167	0.0627	0.092899	0.099199	0.045312
UPPER LIMIT=	15.43912	14.10911	14.02131	14.02804	13.9809	13.87758
LOWER LIMIT=	15.14982	13.84278	13.89591	13.84224	13.78251	13.78695
MEAN Cd =	0.596421	0.545004	0.544328	0.543413	0.541329	0.539401
Cd STD.DEV.=	0.001773	0.001632	0.000768	0.001138	0.001216	0.000555
3.182*STD.DEV.=	0.005641	0.005193	0.002445	0.003623	0.003868	0.001767
UPPER LIMIT=	0.602062	0.550197	0.546773	0.547035	0.545198	0.541168
LOWER LIMIT=	0.59078	0.539811	0.541883	0.53979	0.537461	0.537634

MODEL AOA=	22					
CANARD AOA=	10					
AMPLITUDE=	5					
DELTA P (cm. H2O)=	12					
q (lbf/ft^2)=	27.33					
S (ft^2)=	0.9383					
MAC (in.)=	5.38					
VELOCITY (ft/s)=	151.6454					
FREQUENCY						
Hz=	0	5	10	15	20	25
k=	0	0.046439	0.092877	0.139316	0.185754	0.232193
LIFT						
MEAN LIFT =	36.62231	36.36716	36.29466	36.22689	36.07224	35.88985
STD. DEV.=	0.098204	0.10608	0.062177	0.02764	0.079517	0.070398
3.182*STD.DEV.=	0.312486	0.337547	0.197846	0.087952	0.253024	0.224008
UPPER LIMIT=	36.93479	36.70471	36.49251	36.31484	36.32527	36.11385
LOWER LIMIT=	36.30982	36.02962	36.09682	36.13894	35.81922	35.66584
MEAN Cl =	1.428119	1.418169	1.415342	1.412699	1.406669	1.399556
Cl STD.DEV.=	0.00383	0.004137	0.002425	0.001078	0.003101	0.002745
3.182*STD.DEV.=	0.012186	0.013163	0.007715	0.00343	0.009867	0.008735
UPPER LIMIT=	1.440304	1.431332	1.423057	1.416129	1.416535	1.408291
LOWER LIMIT=	1.415933	1.405006	1.407627	1.409269	1.396802	1.390821
DRAG						
MEAN DRAG =	15.49127	15.2925	15.22074	15.16547	15.15166	15.10235
STD. DEV.=	0.034806	0.033264	0.024964	0.015401	0.035523	0.022888
3.182*STD.DEV.=	0.110751	0.105847	0.079437	0.049006	0.113034	0.07283
UPPER LIMIT=	15.60203	15.39835	15.30017	15.21447	15.2647	15.17518
LOWER LIMIT=	15.38052	15.18666	15.1413	15.11646	15.03863	15.02952
MEAN Cd =	0.604096	0.596344	0.593546	0.591391	0.590852	0.588929
Cd STD.DEV.=	0.001357	0.001297	0.000974	0.000601	0.001385	0.000893
3.182*STD.DEV.=	0.004319	0.004128	0.003098	0.001911	0.004408	0.00284
UPPER LIMIT=	0.608415	0.600472	0.596644	0.593302	0.59526	0.5917
LOWER LIMIT=	0.599777	0.592217	0.590448	0.58948	0.586444	0.586089

MODEL AOA=	22					
CANARD AOA=	4					
AMPLITUDE=	10					
DELTA P (cm. H2O)=	12					
q (lbf/ft^2)=	27.33					
S (ft^2)=	0.9383					
MAC (in.)=	5.38					
VELOCITY (ft/s)=	151.6454					
FREQUENCY						
Hz=	0	5	10	15	20	25
k=	0	0.046439	0.092877	0.139316	0.185754	0.232193
LIFT						
MEAN LIFT =	36.88612	35.62986	35.46336	35.28321	35.09569	34.84926
STD. DEV.=	0.095674	0.114501	0.081638	0.076915	0.121743	0.133334
3.182*STD.DEV.=	0.304434	0.364342	0.259771	0.244742	0.387385	0.424269
UPPER LIMIT=	37.19056	35.99421	35.72314	35.52795	35.48308	35.27353
LOWER LIMIT=	36.58169	35.26552	35.20359	35.03847	34.70831	34.42499
MEAN Cl =	1.438407	1.389418	1.382925	1.3759	1.368587	1.358977
Cl STD.DEV.=	0.003731	0.004465	0.003184	0.002999	0.004747	0.005199
3.182*STD.DEV.=	0.011872	0.014208	0.01013	0.009544	0.015106	0.016545
UPPER LIMIT=	1.450278	1.403626	1.393055	1.385444	1.383694	1.375522
LOWER LIMIT=	1.426535	1.37521	1.372795	1.366356	1.353481	1.342432
DRAG						
MEAN DRAG =	14.80508	14.65584	14.49997	14.42417	14.34867	14.33285
STD. DEV.=	0.036154	0.090177	0.021084	0.01613	0.05073	0.047953
3.182*STD.DEV.=	0.115043	0.286943	0.067089	0.051324	0.161422	0.152585
UPPER LIMIT=	14.92012	14.94278	14.56705	14.47549	14.51009	14.48543
LOWER LIMIT=	14.69003	14.3689	14.43288	14.37284	14.18725	14.18026
MEAN Cd =	0.577337	0.571517	0.565439	0.562483	0.559539	0.558922
Cd STD.DEV.=	0.00141	0.003517	0.000822	0.000629	0.001978	0.00187
3.182*STD.DEV.=	0.004486	0.01119	0.002616	0.002001	0.006295	0.00595
UPPER LIMIT=	0.581823	0.582707	0.568055	0.564484	0.565834	0.564872
LOWER LIMIT=	0.572851	0.560328	0.562823	0.560482	0.553244	0.552972

MODEL AOA=	22					
CANARD AOA=	7					
AMPLITUDE=	10					
DELTA P (cm. H2O)=	12					
q (lbf/ft ²)=	27.33					
S (ft ²)=	0.9383					
MAC (in.)=	5.38					
VELOCITY (ft/s)=	151.6454					
FREQUENCY						
Hz=	0	5	10	15	20	25
k=	0	0.046439	0.092877	0.139316	0.185754	0.232193
LIFT						
MEAN LIFT =	36.73228	35.88776	36.04243	35.80814	35.8319	35.53759
STD. DEV.=	0.108599	0.049705	0.080019	0.18945	0.090697	0.115997
3.182*STD.DEV.=	0.345563	0.158161	0.254619	0.602829	0.288599	0.369102
UPPER LIMIT=	37.07784	36.04592	36.29704	36.41097	36.1205	35.90669
LOWER LIMIT=	36.38672	35.7296	35.78781	35.20531	35.5433	35.16848
MEAN Cl =	1.432407	1.399474	1.405506	1.39637	1.397296	1.385819
Cl STD.DEV.=	0.004235	0.001938	0.00312	0.007388	0.003537	0.004523
3.182*STD.DEV.=	0.013476	0.006168	0.009929	0.023508	0.011254	0.014393
UPPER LIMIT=	1.445883	1.405642	1.415435	1.419878	1.40855	1.400213
LOWER LIMIT=	1.418932	1.393307	1.395577	1.372862	1.386042	1.371426
DRAG						
MEAN DRAG =	15.29447	15.19198	15.07596	14.9812	14.95057	14.84014
STD. DEV.=	0.045459	0.029384	0.02954	0.063397	0.034871	0.050554
3.182*STD.DEV.=	0.14465	0.093501	0.093996	0.201729	0.110958	0.160864
UPPER LIMIT=	15.43912	15.28548	15.16996	15.18293	15.06152	15.001
LOWER LIMIT=	15.14982	15.09848	14.98196	14.77947	14.83961	14.67927
MEAN Cd =	0.596421	0.592425	0.5879	0.584205	0.58301	0.578704
Cd STD.DEV.=	0.001773	0.001146	0.001152	0.002472	0.00136	0.001971
3.182*STD.DEV.=	0.005641	0.003646	0.003665	0.007867	0.004327	0.006273
UPPER LIMIT=	0.602062	0.596071	0.591566	0.592072	0.587337	0.584977
LOWER LIMIT=	0.59078	0.588779	0.584235	0.576338	0.578683	0.572431

MODEL AOA=	22					
CANARD AOA=	10					
AMPLITUDE=	10					
DELTA P (cm. H2O)=	12					
q (lbf/ft ²)=	27.33					
S (ft ²)=	0.9383					
MAC (in.)=	5.38					
VELOCITY (ft/s)=	151.6454					
FREQUENCY						
Hz=	0	5	10	15	20	25
k=	0	0.046439	0.092877	0.139316	0.185754	0.232193
LIFT						
MEAN LIFT =	36.62231	34.80994	35.27483	35.19917	35.04032	34.92356
STD. DEV.=	0.098204	0.139066	0.069301	0.06708	0.022025	0.067171
3.182*STD.DEV.=	0.312486	0.442508	0.220516	0.213448	0.070084	0.213738
UPPER LIMIT=	36.93479	35.25245	35.49535	35.41261	35.1104	35.1373
LOWER LIMIT=	36.30982	34.36743	35.05432	34.98572	34.97023	34.70982
MEAN Cl =	1.428119	1.357444	1.375573	1.372622	1.366428	1.361875
Cl STD.DEV.=	0.00383	0.005423	0.002702	0.002616	0.000859	0.002619
3.182*STD.DEV.=	0.012186	0.017256	0.008599	0.008324	0.002733	0.008335
UPPER LIMIT=	1.440304	1.3747	1.384172	1.380946	1.369161	1.37021
LOWER LIMIT=	1.415933	1.340188	1.366974	1.364299	1.363695	1.35354
DRAG						
MEAN DRAG =	15.39537	15.10609	15.08536	15.09592	15.05513	15.01974
STD. DEV.=	0.157002	0.063047	0.025511	0.024043	0.014435	0.036104
3.182*STD.DEV.=	0.49958	0.200617	0.081177	0.076506	0.045933	0.114883
UPPER LIMIT=	15.89495	15.30671	15.16654	15.17242	15.10107	15.13462
LOWER LIMIT=	14.89579	14.90548	15.00418	15.01941	15.0092	14.90485
MEAN Cd =	0.600356	0.589075	0.588267	0.588679	0.587088	0.585708
Cd STD.DEV.=	0.006122	0.002459	0.000995	0.000938	0.000563	0.001408
3.182*STD.DEV.=	0.019482	0.007823	0.003166	0.002983	0.001791	0.00448
UPPER LIMIT=	0.619837	0.596899	0.591432	0.591662	0.588879	0.590188
LOWER LIMIT=	0.580874	0.581252	0.585101	0.585695	0.585297	0.581228

MODEL AOA=	34					
CANARD AOA=	-4					
AMPLITUDE=	5					
DELTA P (cm. H2O)=	12					
q (lbf/ft ²)=	27.33					
S (ft ²)=	0.9383					
MAC (in.)=	5.38					
VELOCITY (ft/s)=	151.6454					
FREQUENCY						
Hz=	0	5	10	15	20	25
k=	0	0.046439	0.092877	0.139316	0.185754	0.232193
LIFT						
MEAN LIFT =	41.7219	41.96594	42.09249	41.72075	41.57605	41.58474
STD. DEV.=	0.255063	0.093203	0.140407	0.105792	0.102142	0.146297
3.182*STD.DEV.=	0.811609	0.296573	0.446774	0.33663	0.325015	0.465516
UPPER LIMIT=	42.53351	42.26251	42.53926	42.05738	41.90106	42.05025
LOWER LIMIT=	40.9103	41.66936	41.64571	41.38412	41.25103	41.11922
MEAN Cl =	1.626982	1.636498	1.641433	1.626937	1.621294	1.621633
Cl STD.DEV.=	0.009946	0.003635	0.005475	0.004125	0.003983	0.005705
3.182*STD.DEV.=	0.031649	0.011565	0.017422	0.013127	0.012674	0.018153
UPPER LIMIT=	1.658631	1.648064	1.658856	1.640064	1.633969	1.639786
LOWER LIMIT=	1.595333	1.624933	1.624011	1.61381	1.60862	1.60348
DRAG						
MEAN DRAG =	28.39872	28.26335	28.30194	28.12068	28.10789	28.09581
STD. DEV.=	0.108491	0.033945	0.066198	0.05729	0.052261	0.052003
3.182*STD.DEV.=	0.345218	0.108013	0.210641	0.182297	0.166294	0.165475
UPPER LIMIT=	28.74393	28.37136	28.51258	28.30298	28.27418	28.26128
LOWER LIMIT=	28.0535	28.15534	28.0913	27.93838	27.9416	27.93033
MEAN Cd =	1.107433	1.102154	1.103659	1.09659	1.096092	1.095621
Cd STD.DEV.=	0.004231	0.001324	0.002521	0.002234	0.002038	0.002028
3.182*STD.DEV.=	0.013462	0.004212	0.008214	0.007109	0.006485	0.006453
UPPER LIMIT=	1.120895	1.106366	1.111873	1.103699	1.102576	1.102073
LOWER LIMIT=	1.093971	1.097942	1.095445	1.089482	1.089607	1.089168

MODEL AOA=	34					
CANARD AOA=	-7					
AMPLITUDE=	5					
DELTA P (cm. H2O)=	12					
q (lbf/ft ²)=	27.33					
S (ft ²)=	0.9383					
MAC (in.)=	5.38					
VELOCITY (ft/s)=	151.6454					
FREQUENCY						
Hz=	0	5	10	15	20	25
k=	0	0.046439	0.092877	0.139316	0.185754	0.232193
LIFT						
MEAN LIFT =	43.24928	42.15297	42.23697	42.16644	42.14693	41.85903
STD. DEV.=	0.152075	0.211123	0.163877	0.139068	0.037684	0.145572
3.182*STD.DEV.=	0.483902	0.671792	0.521455	0.442515	0.119912	0.463211
UPPER LIMIT=	43.73318	42.82476	42.75842	42.60895	42.26684	42.32224
LOWER LIMIT=	42.76537	41.48118	41.71551	41.72392	42.02702	41.39582
MEAN Cl =	1.686543	1.643792	1.647067	1.644317	1.643556	1.632329
Cl STD.DEV.=	0.00593	0.008233	0.006391	0.005423	0.00147	0.005677
3.182*STD.DEV.=	0.01887	0.026197	0.020335	0.017256	0.004676	0.018063
UPPER LIMIT=	1.705413	1.669989	1.667402	1.661573	1.648232	1.650393
LOWER LIMIT=	1.667673	1.617595	1.626733	1.627061	1.63888	1.614266
DRAG						
MEAN DRAG =	28.14131	27.77621	27.7543	27.69721	27.71591	27.5449
STD. DEV.=	0.026412	0.105301	0.092813	0.08688	0.007353	0.072445
3.182*STD.DEV.=	0.084044	0.335068	0.295332	0.276451	0.023398	0.230519
UPPER LIMIT=	28.22536	28.11128	28.04963	27.97366	27.73931	27.77542
LOWER LIMIT=	28.05727	27.44114	27.45896	27.42076	27.69251	27.31438
MEAN Cd =	1.097395	1.083158	1.082303	1.080077	1.080806	1.074137
Cd STD.DEV.=	0.00103	0.004106	0.003619	0.003388	0.000287	0.002825
3.182*STD.DEV.=	0.003277	0.013066	0.011517	0.01078	0.000912	0.008989
UPPER LIMIT=	1.100672	1.096224	1.09382	1.090857	1.081718	1.083127
LOWER LIMIT=	1.094118	1.070091	1.070786	1.069296	1.079894	1.065148

MODEL AOA=	34					
CANARD AOA=	-10					
AMPLITUDE=	5					
DELTA P (cm. H2O)=	12					
q (lbf/ft^2)=	27.33					
S (ft^2)=	0.9383					
MAC (in.)=	5.38					
VELOCITY (ft/s)=	151.6454					
FREQUENCY						
Hz=	0	5	10	15	20	25
k=	0	0.046439	0.092877	0.139316	0.185754	0.232193
LIFT						
MEAN LIFT =	42.40407	41.79588	41.92224	41.78692	41.88277	41.62126
STD. DEV.=	0.059618	0.136226	0.160787	0.158283	0.055838	0.023508
3.182*STD.DEV.=	0.189706	0.43347	0.511623	0.503657	0.177678	0.074802
UPPER LIMIT=	42.59378	42.22935	42.43386	42.29057	42.06044	41.69606
LOWER LIMIT=	42.21437	41.36241	41.41062	41.28326	41.70509	41.54646
MEAN Cl =	1.653584	1.629867	1.634794	1.629517	1.633255	1.623057
Cl STD.DEV.=	0.002325	0.005312	0.00627	0.006172	0.002177	0.000917
3.182*STD.DEV.=	0.007398	0.016904	0.019951	0.019641	0.006929	0.002917
UPPER LIMIT=	1.660982	1.64677	1.654746	1.649158	1.640184	1.625974
LOWER LIMIT=	1.646186	1.612963	1.614843	1.609877	1.626326	1.620141
DRAG						
MEAN DRAG =	27.32982	26.89041	26.93577	26.84227	26.93257	26.75407
STD. DEV.=	0.033418	0.075427	0.074768	0.091834	0.02875	0.015526
3.182*STD.DEV.=	0.106336	0.240008	0.237913	0.292216	0.091482	0.049403
UPPER LIMIT=	27.43616	27.13041	27.17368	27.13449	27.02405	26.80348
LOWER LIMIT=	27.22348	26.6504	26.69786	26.55005	26.84109	26.70467
MEAN Cd =	1.06575	1.048615	1.050384	1.046738	1.050259	1.043298
Cd STD.DEV.=	0.001303	0.002941	0.002916	0.003581	0.001121	0.000605
3.182*STD.DEV.=	0.004147	0.009359	0.009278	0.011395	0.003567	0.001927
UPPER LIMIT=	1.069897	1.057974	1.059661	1.058133	1.053827	1.045225
LOWER LIMIT=	1.061604	1.039256	1.041106	1.035343	1.046692	1.041372

MODEL AOA=	34					
CANARD AOA=	-4					
AMPLITUDE=	10					
DELTA P (cm. H2O)=	12					
q (lbf/ft ²)=	27.33					
S (ft ²)=	0.9383					
MAC (in.)=	5.38					
VELOCITY (ft/s)=	151.6454					
FREQUENCY						
Hz=	0	5	10	15	20	25
k=	0	0.046439	0.092877	0.139316	0.185754	0.232193
LIFT						
MEAN LIFT =	41.7219	41.68476	41.61744	41.4616	41.51339	41.33265
STD. DEV.=	0.255063	0.045258	0.119078	0.037197	0.117325	0.127482
3.182*STD.DEV.=	0.811609	0.144012	0.378907	0.11836	0.373328	0.405648
UPPER LIMIT=	42.53351	41.82877	41.99635	41.57996	41.88671	41.7383
LOWER LIMIT=	40.9103	41.54074	41.23854	41.34324	41.14006	40.927
MEAN CL =	1.626982	1.625533	1.622909	1.616831	1.618851	1.611803
CL STD.DEV.=	0.009946	0.001765	0.004644	0.001451	0.004575	0.004971
3.182*STD.DEV.=	0.031649	0.005616	0.014776	0.004616	0.014558	0.015819
UPPER LIMIT=	1.658631	1.631149	1.637684	1.621447	1.633409	1.627621
LOWER LIMIT=	1.595333	1.619918	1.608133	1.612216	1.604292	1.595984
DRAG						
MEAN DRAG =	28.39872	28.09699	27.85282	27.76555	27.74751	27.67066
STD. DEV.=	0.108491	0.026359	0.051637	0.027289	0.053095	0.062103
3.182*STD.DEV.=	0.345218	0.083873	0.16431	0.086833	0.168949	0.197612
UPPER LIMIT=	28.74393	28.18087	28.01713	27.85239	27.91646	27.86827
LOWER LIMIT=	28.0535	28.01312	27.68851	27.67872	27.57856	27.47305
MEAN Cd =	1.107433	1.095667	1.086145	1.082742	1.082038	1.079042
Cd STD.DEV.=	0.004231	0.001028	0.002014	0.001064	0.00207	0.002422
3.182*STD.DEV.=	0.013462	0.003271	0.006407	0.003386	0.006588	0.007706
UPPER LIMIT=	1.120895	1.098937	1.092553	1.086128	1.088627	1.0867
LOWER LIMIT=	1.093971	1.092396	1.079738	1.079356	1.07545	1.071336

MODEL AOA=	34					
CANARD AOA=	-7					
AMPLITUDE=	10					
DELTA P (cm. H2O)=	12					
q (lbf/ft^2)=	27.33					
S (ft^2)=	0.9383					
MAC (in.)=	5.38					
VELOCITY (ft/s)=	151.6454					
FREQUENCY						
Hz=	0	5	10	15	20	25
k=	0	0.046439	0.092877	0.139316	0.185754	0.232193
LIFT						
MEAN LIFT =	43.25268	41.06015	41.09099	41.15339	41.01945	41.12252
STD. DEV.=	0.14652	0.10197	0.093618	0.151984	0.072549	0.161978
3.182*STD.DEV.=	0.466227	0.324469	0.297892	0.483613	0.230852	0.515414
UPPER LIMIT=	43.71891	41.38462	41.38888	41.637	41.25031	41.63794
LOWER LIMIT=	42.78645	40.73568	40.7931	40.66977	40.7886	40.60711
MEAN Cl =	1.686676	1.601176	1.602379	1.604812	1.599589	1.603609
Cl STD.DEV.=	0.005714	0.003976	0.003651	0.005927	0.002829	0.006316
3.182*STD.DEV.=	0.018181	0.012653	0.011617	0.018859	0.009002	0.020099
UPPER LIMIT=	1.704857	1.613829	1.613996	1.623671	1.608592	1.623708
LOWER LIMIT=	1.668495	1.588523	1.590762	1.585953	1.590587	1.58351
DRAG						
MEAN DRAG =	28.14131	27.4693	27.24352	27.30029	27.29642	27.31911
STD. DEV.=	0.026412	0.059916	0.064487	0.077418	0.044499	0.083987
3.182*STD.DEV.=	0.084044	0.190654	0.205199	0.246346	0.141597	0.267247
UPPER LIMIT=	28.22536	27.65995	27.44872	27.54664	27.43802	27.58636
LOWER LIMIT=	28.05727	27.27864	27.03833	27.05395	27.15482	27.05186
MEAN Cd =	1.097395	1.071189	1.062385	1.064599	1.064448	1.065333
Cd STD.DEV.=	0.00103	0.002336	0.002515	0.003019	0.001735	0.003275
3.182*STD.DEV.=	0.003277	0.007435	0.008002	0.009606	0.005522	0.010422
UPPER LIMIT=	1.100672	1.078624	1.070387	1.074205	1.069969	1.075754
LOWER LIMIT=	1.094118	1.063755	1.054383	1.054992	1.058926	1.054911

MODEL AOA=	34					
CANARD AOA=	-10					
AMPLITUDE=	10					
DELTA P (cm. H2O)=	12					
q (lb/ft ²)=	27.33					
S (ft ²)=	0.9383					
MAC (in.)=	5.38					
VELOCITY (ft/s)=	151.6454					
FREQUENCY						
Hz=	0	5	10	15	20	25
k=	0	0.046439	0.092877	0.139316	0.185754	0.232193
LIFT						
MEAN LIFT =	42.40407	41.63824	41.53664	41.77239	41.56922	41.6576
STD. DEV.=	0.059618	0.15827	0.120164	0.061498	0.082291	0.093878
3.182*STD.DEV.=	0.189706	0.503615	0.382363	0.195687	0.261851	0.298721
UPPER LIMIT=	42.59377	42.14185	41.919	41.96808	41.83107	41.95632
LOWER LIMIT=	42.21437	41.13462	41.15428	41.57671	41.30736	41.35888
MEAN Cl =	1.653584	1.623719	1.619758	1.628951	1.621028	1.624474
Cl STD.DEV.=	0.002325	0.006172	0.004686	0.002398	0.003209	0.003661
3.182*STD.DEV.=	0.007398	0.019639	0.014911	0.007631	0.010211	0.011649
UPPER LIMIT=	1.660982	1.643358	1.634668	1.636582	1.631239	1.636123
LOWER LIMIT=	1.646186	1.60408	1.604847	1.62132	1.610817	1.612826
DRAG						
MEAN DRAG =	27.32982	27.57928	27.31677	27.45698	27.4311	27.45643
STD. DEV.=	0.033418	0.10223	0.064667	0.031294	0.048506	0.043012
3.182*STD.DEV.=	0.106336	0.325295	0.20577	0.099577	0.154346	0.136864
UPPER LIMIT=	27.43616	27.90457	27.52254	27.55655	27.58545	27.5933
LOWER LIMIT=	27.22348	27.25398	27.111	27.3574	27.27675	27.31957
MEAN Cd =	1.06575	1.075478	1.065241	1.070709	1.0697	1.070688
Cd STD.DEV.=	0.001303	0.003987	0.002522	0.00122	0.001892	0.001677
3.182*STD.DEV.=	0.004147	0.012685	0.008024	0.003883	0.006019	0.005337
UPPER LIMIT=	1.069897	1.088163	1.073266	1.074592	1.075719	1.076025
LOWER LIMIT=	1.061604	1.062793	1.057217	1.066826	1.063681	1.06535

INITIAL DISTRIBUTION LIST

1. Defense Technical Information Center 2
Cameron Station
Alexandria, Va 22304-6145
2. Library, Code 52 2
Naval Postgraduate School
Monterey, Ca 93943-5002
3. Professor Daniel J. Collins, Code AA/Co 1
Chairman,
Department of Aeronautics and Astronautics
Naval Postgraduate School
Monterey, Ca 93943-5000
4. Michael J. Harris 1
Code AIR-530TA
Naval Air Systems Command
Washington, DC 20361
5. Professor Richard M. Howard, Code AA/Ho 2
Naval Postgraduate School
Monterey, Ca 93943-5000
6. Professor Maximilian F. Platzer 2
Naval Postgraduate School
Monterey, Ca 93943-5000
7. LT Douglas G. Mc Bane 2
1277 Leahy Rd.
Monterey, Ca 93940